Spring 2018 – Systems Biology of Reproduction
Discussion Outline – Testis Systems Biology
Michael K. Skinner – Biol 475/575
CUE 418, 10:35-11:50 am, Tuesday & Thursday
February 22, 2018
Week 7

Testis Systems Biology

Primary Papers:

1. Endo, et al. (2015) PNAS E2347-2356
2. Chalmel, et al., (2014) Plos One 9:e104418
3. Gatta, et al. (2010) BMC Genomics 11:401

Discussion

Student 19: Reference 1 above

- How do retinoids and Stra8 interact?
- What experimental design was used?
- What is the integration of retinoid actions and spermatogenesis?

Student 20: Reference 2 above

- What was the experimental design and omics technologies used?
- What was the secretome observed?
- How do Sertloli and germ cells interact?

Student 22: Reference 3 above

- What is the experimental and systems approach?
- What genetic and expression relationships exist?
- What insights are provided on the molecular control of male infertility?

Periodic retinoic acid–STRA8 signaling intersects with periodic germ-cell competencies to regulate spermatogenesis

Tsutomu Endo[a,1,2], Katherine A. Romer[a,b,1], Ericka L. Anderson[a,c,1], Andrew E. Baltus[a,c], Dirk G. de Rooij[a], and David C. Page[a,c,d,2]

[a]Whitehead Institute, Cambridge, MA 02142; [b]Computational and Systems Biology Program and [c]Department of Biology, Massachusetts Institute of Technology, Cambridge, MA 02139; and [d]Howard Hughes Medical Institute, Whitehead Institute, Cambridge, MA 02142

Contributed by David C. Page, March 24, 2015 (sent for review January 18, 2015; reviewed by William W. Wright)

Mammalian spermatogenesis—the transformation of stem cells into millions of haploid spermatozoa—is elaborately organized in time and space. We explored the underlying regulatory mechanisms by genetically and chemically perturbing spermatogenesis in vivo, focusing on spermatogonial differentiation, which begins a series of amplifying divisions, and meiotic initiation, which ends these divisions. We first found that, in mice lacking the retinoic acid (RA) target gene *Stimulated by retinoic acid gene 8* (*Stra8*), undifferentiated spermatogonia accumulated in unusually high numbers as early as 10 d after birth, whereas differentiating spermatogonia were depleted. We thus conclude that *Stra8*, previously shown to be required for meiotic initiation, also promotes (but is not strictly required for) spermatogonial differentiation. Second, we found that injection of RA into wild-type adult males induced, independently, precocious spermatogonial differentiation and precocious meiotic initiation; thus, RA acts instructively on germ cells at both transitions. Third, the competencies of germ cells to undergo spermatogonial differentiation or meiotic initiation in response to RA were found to be distinct, periodic, and limited to particular seminiferous stages. Competencies for both transitions begin while RA levels are low, so that the germ cells respond as soon as RA levels rise. Together with other findings, our results demonstrate that periodic RA–STRA8 signaling intersects with periodic germ-cell competencies to regulate two distinct, cell-type-specific responses: spermatogonial differentiation and meiotic initiation. This simple mechanism, with one signal both starting and ending the amplifying divisions, contributes to the prodigious output of spermatozoa and to the elaborate organization of spermatogenesis.

spermatogenesis | Stra8 | mouse | retinoic acid | testis

The adult mammalian testis is among the body's most proliferative tissues, producing millions of highly specialized gametes, or spermatozoa, each day. Spermatogenesis (the program of sperm production) is carefully regulated, ensuring that spermatozoa are produced at a constant rate. We used the mouse as a model to understand how mammalian spermatogenesis is organized at the cellular and molecular level. We focused on two key transitions: spermatogonial differentiation, which occurs cyclically and begins a series of programmed mitotic divisions, and meiotic initiation, which ends these divisions and marks the beginning of the meiotic program (Fig. 1*A*).

Like other proliferative tissues (e.g., blood, intestine, and skin), the testis relies on a modest number of stem cells (1, 2). The undifferentiated spermatogonia (also known as the A_{single}/A_{paired}/$A_{aligned}$ spermatogonia), which encompass these stem cells, have a remarkable capacity for self-renewal and differentiation: They can reconstitute spermatogenesis upon transplantation to a germ-cell-depleted testis (3, 4). In vivo, undifferentiated spermatogonia ultimately give rise to a single cell type, spermatozoa, yet these undifferentiated spermatogonia express pluripotency-associated genes such as *Lin28a* (*Lin-28 homolog A*) (5) and *Pou5f*/*Oct4* (6, 7) and are the only postnatal mammalian cells from which functionally pluripotent cells have been derived in vitro without introduction of exogenous transcription factors or miRNAs (8). Undifferentiated spermatogonia periodically undergo spermatogonial differentiation (also known as the $A_{aligned}$-to-A_1 transition) to become differentiating spermatogonia (also known as A_1/A_2/A_3/A_4/intermediate/B spermatogonia). During spermatogonial differentiation, the spermatogonia down-regulate pluripotency-associated genes (5, 9), lose capacity for self-renewal (4), and accelerate their cell cycle (10) to begin a series of six transit-amplifying mitotic ivisions. At the conclusion of these mitotic divisions, germ cells become spermatocytes, and undergo meiotic initiation (Fig. 1*A*). This begins the meiotic program of DNA replication and reductive cell divisions, ensuring that spermatozoa contribute exactly one of each chromosome to the zygote.

Meiotic initiation is precisely coordinated with spermatogonial differentiation: The six mitotic divisions separating the two transitions occur over a span of exactly 8.6 d (11). Moreover, spermatogonial differentiation and meiotic initiation occur in close physical proximity. The testis comprises structures known as seminiferous tubules (Fig. S1*A*); while one generation of germ cells is initiating meiosis, a younger generation is simultaneously undergoing spermatogonial differentiation, within the same tubule

Significance

As male sex cells mature into sperm, two pivotal transitions are spermatogonial differentiation (exit from the stem cell pool) and meiotic initiation. These transitions occur in physical proximity, with 8.6-d periodicity. We report that the gene *Stra8*, essential for meiotic initiation, also promotes (but is not required for) spermatogonial differentiation. Moreover, injected RA induces both transitions to occur precociously. We conclude that a periodic RA signal, acting instructively through the common target *Stra8*, coordinates these transitions. This RA signal intersects with two distinct windows of sex-cell competency, which both begin while RA levels are low; sex cells respond quickly to rising RA. These mechanisms help account for the elaborate organization of sperm production, and its prodigious output.

Author contributions: T.E., K.A.R., E.L.A., D.G.d.R., and D.C.P. designed research; T.E., K.A.R., E.L.A., and A.E.B. performed research; T.E., K.A.R., E.L.A., and D.G.d.R. analyzed data; and T.E., K.A.R., and D.C.P. wrote the paper.

Reviewers included: W.W.W., Johns Hopkins Bloomberg School of Public Health.

The authors declare no conflict of interest.

Data deposition: The mRNA-sequencing dataset reported in this paper has been deposited in the Gene Expression Omnibus (GEO) database, www.ncbi.nlm.nih.gov/geo (accession no. GSE67169).

[1]T.E., K.A.R, and E.L.A. contributed equally to this work.

[2]To whom correspondence may be addressed. Email: endo@wi.mit.edu or dcpage@wi.mit.edu.

This article contains supporting information online at www.pnas.org/lookup/suppl/doi:10.1073/pnas.1505683112/-/DCSupplemental.

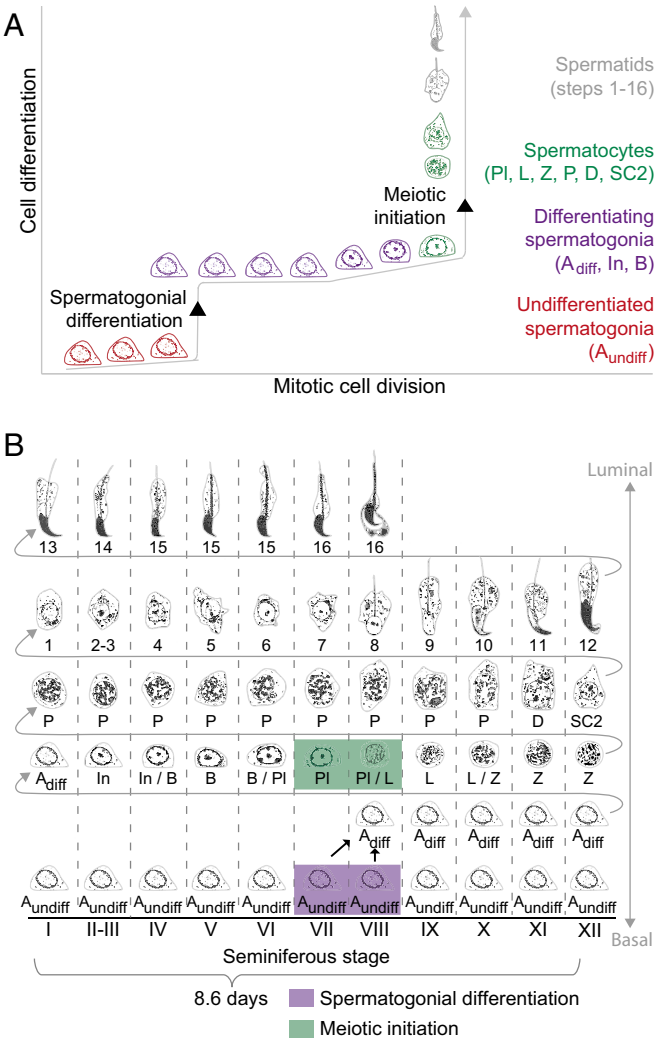

Fig. 1. Overview of spermatogenesis. (*A*) Diagram of mouse spermatogenesis. Germ cells develop from undifferentiated, mitotic spermatogonia (red, bottom left), to differentiating spermatogonia (purple, middle left), to spermatocytes (germ cells that undergo meiosis, green, middle right), to haploid spermatids (gray, top right). We highlight two cellular differentiation steps: spermatogonial differentiation and meiotic initiation. (*B*) Diagram of germ-cell associations (stages) in the mouse testis. Oakberg (33) identified 12 distinct cellular associations, called seminiferous stages I–XII. In the mouse, it takes 8.6 d for a section of the seminiferous tubule, and the germ cells contained within, to cycle through all 12 stages (41). Four turns of this seminiferous cycle are required for a germ cell to progress from undifferentiated spermatogonium to spermatozoon that is ready to be released into the tubule lumen. A_{undiff}, A_{diff}, In, and B: undifferentiated type A, differentiating type A, intermediate, and type B spermatogonia, respectively. D, L, P, Pl, SC2, and Z: diplotene, leptotene, pachytene, preleptotene, secondary spermatocytes, and zygotene, respectively. Steps 1–16: steps in spermatid differentiation. Purple: germ cells undergoing spermatogonial differentiation; green: meiotic initiation.

cross-section (Fig. 1*B* and Fig. S1*A*). Spermatogonial differentiation and meiotic initiation occur in close association not only in mice but also in other mammals, including rats (12, 13), hamsters, and rams (14). This precise coordination of different steps of spermatogenesis is called the "cycle of the seminiferous epithelium" (or "seminiferous cycle"); it has fascinated biologists for over a century (15). We sought to explain the cooccurrence of spermatogonial differentiation and meiotic initiation, to better understand the regulation of these two transitions and the overall organization of the testis.

Both of these transitions require RA, a derivative of vitamin A. In vitamin A-deficient (VAD) mice and rats, most germ cells arrest as undifferentiated spermatogonia (16, 17). In VAD rat testes, some germ cells instead arrest just before meiosis, as preleptotene spermatocytes (16, 18). When VAD animals are injected with RA or vitamin A, the arrested spermatogonia differentiate (17–19), and the arrested preleptotene spermatocytes initiate meiosis (18). During spermatogonial differentiation, RA is believed to act, at least in part, directly on germ cells: Spermatogonia express RA receptors (RARs) (20), and genetic ablation of RARs in germ cells modestly impairs spermatogonial differentiation (21).

To understand how RA might coregulate these two transitions, we needed to understand its target genes. During meiotic initiation, RA acts instructively, through the target gene *Stra8* (*Stimulated by retinoic acid gene 8*). RA induces *Stra8* expression in germ cells—not in somatic cells—in both males and females (22, 23). *Stra8* is required for meiotic initiation in both sexes: *Stra8*-deficient germ cells in postnatal males and fetal females arrest just before meiosis, without entering meiotic prophase (24, 25). In contrast, no specific RA target genes have been implicated in spermatogonial differentiation: RA could either instruct the germ cells or simply be permissive for this transition. We considered *Stra8* as a candidate regulator of spermatogonial differentiation: STRA8 protein is expressed in spermatogonia as well as in preleptotene spermatocytes in vivo (26, 27), and in vitro studies suggest that RA can act directly on early spermatogonia to increase expression of *Stra8* (28). However, the functional role, if any, of *Stra8* in spermatogonia was not previously known. Using two complementary perturbations of RA–STRA8 signaling—genetic disruption of *Stra8* function and chemical manipulation of RA levels—we demonstrated that RA acts instructively, and at least in part through STRA8, at spermatogonial differentiation as well as at meiotic initiation. The shared RA–STRA8 signal helps to coordinate these two transitions in time and space.

Results

Massive Accumulations of Type A Spermatogonia in Testes of Aged *Stra8*-Deficient Males. As we previously reported, *Stra8*-deficient testes lacked meiotic and postmeiotic cells (24, 25); thus, at 8 wk of age, *Stra8*-deficient testes were much smaller than wild-type testes (25). However, we observed that, after 6 mo, some *Stra8*-deficient testes were grossly enlarged (>400 mg) (44%; 11 of 25 mice) compared with wild-type testes (91 ± 7 mg; average of testes from three mice) (Fig. 2*A*). Both small and large aged *Stra8*-deficient testes (88%; 22 of 25 mice) contained accumulated cells that resembled spermatogonia and expressed the germ-cell marker DAZL (Fig. 2*B*); these accumulations were absent in aged wild-type and heterozygous mice (0%, 0 of 10 mice). In wild-type testes, spermatogonia were confined to the basal lamina of seminiferous tubules, but even in small *Stra8*-deficient testes (<50 mg) occasional tubules were filled with presumptive spermatogonia, which sometimes spilled into the testicular interstitium. Large *Stra8*-deficient testes were composed almost entirely of presumptive spermatogonia, with few remnants of tubule structure. Spermatogonial morphology was very similar between small and large *Stra8*-deficient testes. We used mRNA sequencing (mRNA-Seq) to confirm that spermatogonia had accumulated in *Stra8*-deficient testes; known spermatogonial marker genes (29) were up-regulated in *Stra8*-deficient testes vs. wild-type testes (Fig. S2*A*).

We classified more precisely the spermatogonia in these massive accumulations. Based on nuclear morphology, spermatogonia can be classified as type A, intermediate, or type B (Fig. 1 *A* and *B*) (11). Type A includes the undifferentiated and early differentiating spermatogonia, whereas intermediate and type B encompass the later differentiating spermatogonia. The

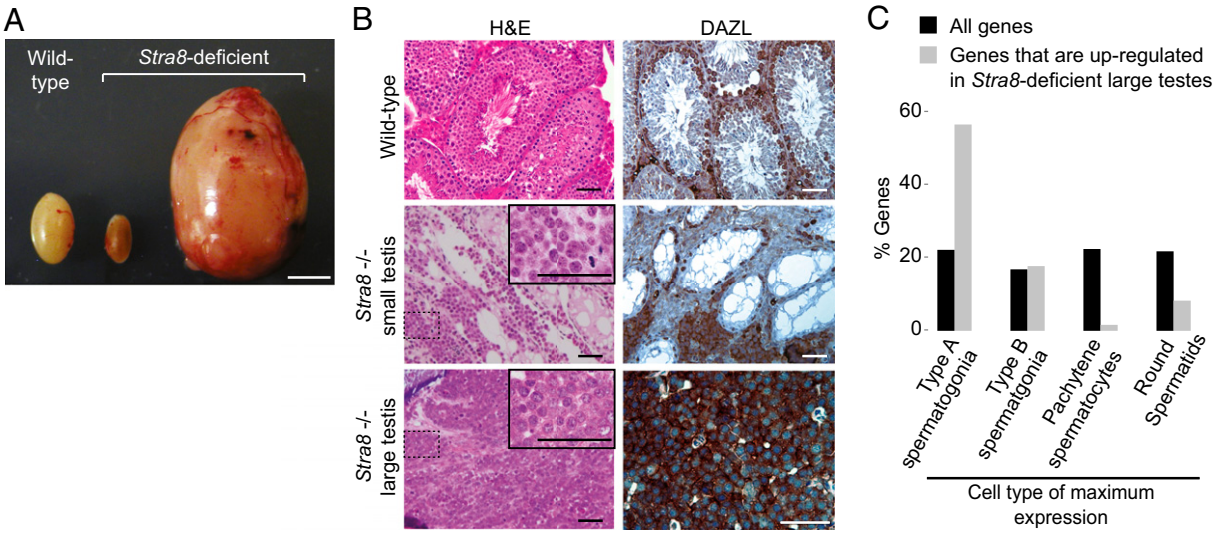

Fig. 2. Aged *Stra8*-deficient testes accumulate type A spermatogonia. (*A*) Wild-type (left) and *Stra8*-deficient small (center) and large (right) testes from 1-y-old mice. (Scale bar, 5 mm.) (*B*) Testis sections from 1-y-old mice: wild-type (*Top*), *Stra8*-deficient small testis (*Middle*), and *Stra8*-deficient grossly enlarged testis (*Bottom*). (*Left*) H&E staining (*Right*) DAZL immunostaining. Insets enlarge the boxed regions. (Scale bars, 50 μm.) (*C*) Percentage of genes whose highest expression is found in type A spermatogonia, type B spermatogonia, pachytene spermatocytes, or round spermatids. Black bars (control), all analyzable genes (17,345 genes). Gray bars, 100 genes most significantly up-regulated in *Stra8*-deficient large testes relative to wild-type testes (Table S1).

Stra8-deficient spermatogonia had type A morphology (Fig. 2*B*). To confirm this, we used mRNA-Seq to identify the 100 genes most significantly up-regulated in *Stra8*-deficient vs. wild-type testes (Table S1). We analyzed their expression among different cell types in wild-type testes, using a published microarray dataset (30); 59% of these 100 genes were most highly expressed in type A spermatogonia, vs. 22.7% of a control gene set (all 17,345 genes on the microarray) (Fig. 2*C*) ($P < 0.001$, Fisher's exact test). A genome-wide clustering analysis of these data and other publically available datasets confirmed that the expression patterns of *Stra8*-deficient testes were overall quite similar to those of type A spermatogonia (Fig. S2*B* and *SI Results and Discussion*). We conclude that type A spermatogonia accumulate in *Stra8*-deficient testes. This suggests that STRA8 has a functional role in type A spermatogonia, distinct from its role in meiotic initiation.

Early Postnatal *Stra8*-Deficient Testes Contain Accumulations of Undifferentiated Spermatogonia and Are Depleted for Differentiating Spermatogonia. We considered our findings in light of published observations that (*i*) a subset of type A spermatogonia undergo spermatogonial differentiation, (*ii*) RA is required for spermatogonial differentiation (17, 18), and (*iii*) RA can act directly on spermatogonia to induce *Stra8* expression (28). We postulated that in the unperturbed wild-type testis, RA induction of *Stra8* promotes spermatogonial differentiation, whereas in the absence of *Stra8*, impaired spermatogonial differentiation leads to accumulation of undifferentiated spermatogonia, accounting for the massive accumulations of type A spermatogonia observed in aged *Stra8*-deficient males.

This hypothesis predicts that even in very young males *Stra8*-deficient testes should contain more undifferentiated spermatogonia than wild-type testes. To test this, we counted undifferentiated spermatogonia in testes from 10-d-old (p10) animals (Fig. 3 *A* and *B* and Fig. S3 *A* and *B*), using the markers LIN28A and PLZF (promyelocytic leukemia zinc finger, a.k.a. ZBTB16) (9, 31). As predicted, LIN28- and PLZF-positive spermatogonia were enriched in *Stra8*-deficient testes ($P < 10^{-15}$ for LIN28A, $P < 10^{-4}$ for PLZF, one-tailed Kolmogorov–Smirnov test) (Fig. 3*B* and Fig. S3*B*). *Stra8*-deficient testes had 9.4 ± 2.3 LIN28A-positive spermatogonia per tubule cross-section, vs. 4.4 ± 0.8 in wild-type testes ($P = 0.026$, one-tailed Welch's *t* test). As the testis matured, the number of undifferentiated spermatogonia per tubule cross-section declined in both wild-type and *Stra8*-deficient testes, but undifferentiated spermatogonia remained significantly enriched in *Stra8*-deficient testes at p30 (Fig. 3*C* and Fig. S3*C*). Indeed, some testis tubules in p30 *Stra8*-deficient mice contained large clusters of LIN28A-positive and PLZF-positive type A spermatogonia (Fig. 3*D* and Fig. S3*E*). Spermatogonia in these clusters were densely packed in multiple layers, whereas in wild-type testes type A spermatogonia were widely spaced in a single layer (Fig. S3*D*). Thus, we conclude that undifferentiated spermatogonia progressively accumulate in *Stra8*-deficient animals. mRNA-Seq and immunohistochemical data from testes of aged *Stra8*-deficient mice were consistent with such an accumulation (Fig. S2 *B–E* and *SI Results and Discussion*).

If this progressive accumulation were due to a defect in spermatogonial differentiation, the proportion of differentiating spermatogonia should be smaller in *Stra8*-deficient testes than in wild-type testes. We thus counted type B (differentiating) spermatogonia in *Stra8*-deficient and wild-type testes at p30 (Fig. 3*C* and Fig. S3*F*). Indeed, compared with wild-type testes, *Stra8*-deficient testes contained significantly fewer type B spermatogonia per tubule cross-section. As predicted, the ratio of differentiating-to-undifferentiated (LIN28-positive) spermatogonia was decreased to 2.8 in *Stra8*-deficient testes, vs. 7.9 in wild-type testes ($P = 0.05$ by Mann–Whitney *U* test). We conclude that STRA8 promotes (but is not strictly required for) spermatogonial differentiation.

STRA8 Expression Begins Shortly Before Spermatogonial Differentiation. Previous reports showed that STRA8 is expressed in spermatogonia and spermatocytes but did not distinguish between different subtypes of spermatogonia (26, 27). We tested our model's prediction that STRA8 must be expressed before or during spermatogonial differentiation, immunostaining intact testis tubules for STRA8 and for PLZF (Fig. 4*A* and Fig. S4*A*). A subset of PLZF-positive (undifferentiated) spermatogonia expressed STRA8. We next immunostained for GFRα1 (GDNF family receptor alpha 1), a marker of early undifferentiated spermatogonia (Fig. S4*A*) (32). GFRα1 did not overlap with STRA8. We thus hypothesized that STRA8 expression begins immediately before spermatogonial differentiation.

To confirm this, we immunostained testis sections for STRA8 and then classified tubules by stage of the cycle of the seminif-

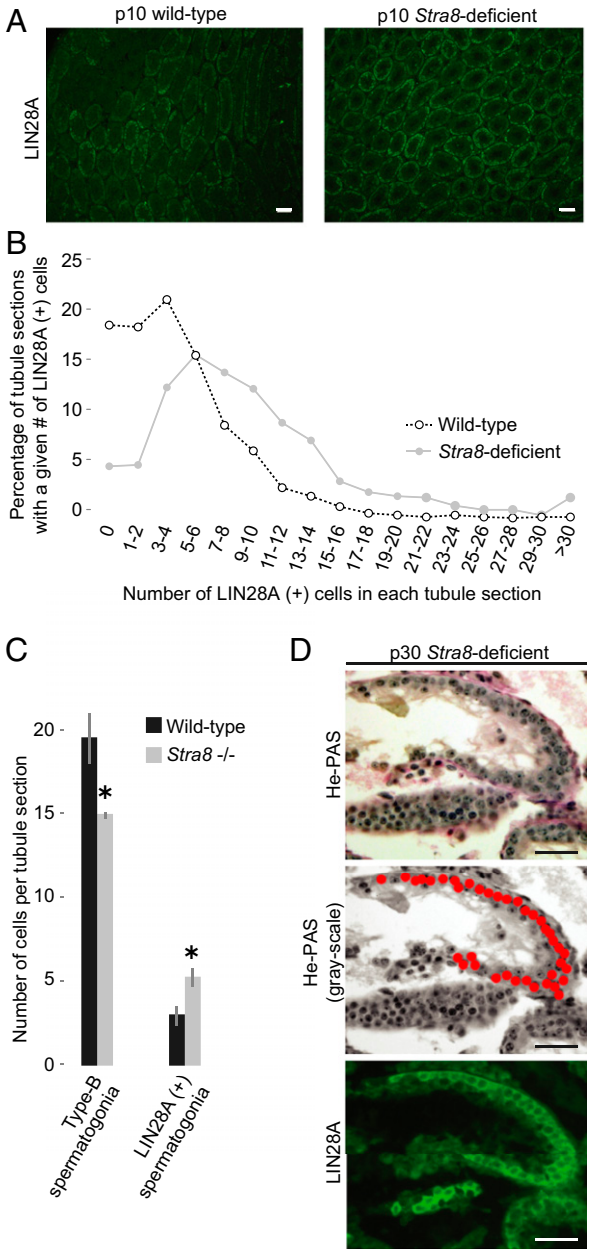

Fig. 3. Testes of young *Stra8*-deficient males are enriched for LIN28A-positive spermatogonia. (*A*) Immunostaining for LIN28A on postnatal day 10 (p10) testis sections: wild-type (*Left*) and *Stra8*-deficient (*Right*). (Scale bars, 50 μm.) (*B*) Histogram of number of LIN28A-positive cells per tubule cross-section, in p10 wild-type and *Stra8*-deficient testes. For each genotype, testes from three mice were counted and averaged. (*C*) Number of type B and LIN28A-positive spermatogonia per tubule cross-section, in p30 wild-type and *Stra8*-deficient testes. Only tubules containing ≥1 type B spermatogonia were counted. Error bars, mean ± SD $*P < 0.01$ (one-tailed Welch's *t* test). (*D*) Clusters of LIN28A-positive undifferentiated spermatogonia in p30 *Stra8*-deficient testes. (*Top*) Hematoxylin and periodic acid-Schiff (He-PAS) staining. (*Middle*) Grayscale version of top panel, with red dots indicating type A spermatogonia. (*Bottom*) LIN28A immunostaining on adjacent section. (Scale bars, 50 μm.)

erous epithelium (hereafter referred to as "seminiferous stage") (Fig. 1*B* and Fig. S1*B*). In the testis, particular germ-cell types are always found in the same tubule cross-section; Oakberg (33) identified 12 such stereotypical associations of germ cells, called stages I–XII. Any given section of a seminiferous tubule cycles through all 12 stages in order, with a full seminiferous cycle encompassing these stages taking 8.6 d. Spermatogonial differentiation and meiotic initiation occur together in stages VII/VIII. Consistent with our hypothesis, STRA8 expression was rare in stages II–VI (before spermatogonial differentiation) then increased rapidly in stages VII–VIII (during spermatogonial differentiation) and remained high thereafter, in stages IX–I (Fig. S1*C*). [Similar increases in STRA8 expression in stage VII or VIII have been previously reported (34, 35)]. We further find that STRA8 expression overlapped with PLZF in stages VII–VIII and was limited to PLZF-low and -negative spermatogonia thereafter, in stages IX–X (Fig. 4 *A* and *B* and Fig. S4*A*). We thus conclude that STRA8 expression begins in late undifferentiated spermatogonia and persists in differentiating spermatogonia.

Intriguingly, in stages VII–VIII, STRA8 expression increased in preleptotene spermatocytes (premeiotic cells) as well as in undifferentiated spermatogonia (Fig. S1 *D* and *E*) (27, 35). Because STRA8 promotes spermatogonial differentiation and is required for meiotic initiation, precisely timed increases in STRA8 expression might coordinate both transitions, ensuring their cooccurrence in stages VII–VIII.

STRA8 expression is induced by RA (22, 23, 26, 28). We hypothesized that RA, acting through *Stra8*, coordinates spermatogonial differentiation with meiotic initiation. To test this, we perturbed RA signaling in the testes of wild-type mice, by injecting either RA or WIN18,446, an inhibitor of RA synthesis (36, 37). We first predicted that injected RA would induce ectopic STRA8 expression both in undifferentiated spermatogonia and in premeiotic cells (differentiating spermatogonia/preleptotene spermatocytes). Furthermore, injected RA should induce both precocious spermatogonial differentiation and precocious meiotic initiation. In contrast, WIN18,446 should inhibit STRA8 expression, spermatogonial differentiation, and meiotic initiation. We proceeded to test these predictions.

Injected RA Induces Precocious STRA8 Expression in Both Undifferentiated Spermatogonia and Premeiotic Germ Cells. We first verified that injected RA induced precocious STRA8 protein expression in the spermatogonial population, which encompasses both undifferentiated spermatogonia and premeiotic cells. In the unperturbed wild-type testis, spermatogonia began to express STRA8 in stages VII–VIII (during spermatogonial differentiation/meiotic initiation) (Fig. 4*C*). At 1 d after RA injection, STRA8 expression was strongly induced in spermatogonia in stages II–VI (Fig. 4*C*), as previously reported (34). In contrast, when we treated mice for 2 d with the RA synthesis inhibitor WIN18,446, spermatogonial STRA8 expression was almost completely eliminated in all stages (Fig. 4 *C* and *D*).

We next showed that injected RA induced precocious STRA8 expression specifically in undifferentiated spermatogonia, by staining testis sections and intact testis tubules for STRA8 and PLZF (Fig. 4 *A*, *B*, and *E* and Fig. S4 *A* and *B*). Indeed, after RA injection, STRA8 expression was strongly induced in a subset of undifferentiated spermatogonia. STRA8 was not induced in any undifferentiated spermatogonia in stages IX–X, but only in late undifferentiated spermatogonia in stages II–VI. We conclude that a very specific subset of undifferentiated spermatogonia is competent to express STRA8.

Finally, we demonstrated that injected RA could induce precocious STRA8 expression in premeiotic cells, which we identified by nuclear morphology and by absence of PLZF expression (Fig. S4*C*). In the unperturbed testis, STRA8 was expressed in preleptotene spermatocytes in stages VII–VIII (during meiotic initiation) but was otherwise absent in premeiotic cells (Fig. 4*F* and Fig. S4*D*). After RA injection, STRA8 was strongly induced in all premeiotic cells, including intermediate and type B spermatogonia and preleptotene spermatocytes, in stages II–VI. We conclude that both undifferentiated spermatogonia and premeiotic cells precociously express STRA8 when exposed to RA in vivo.

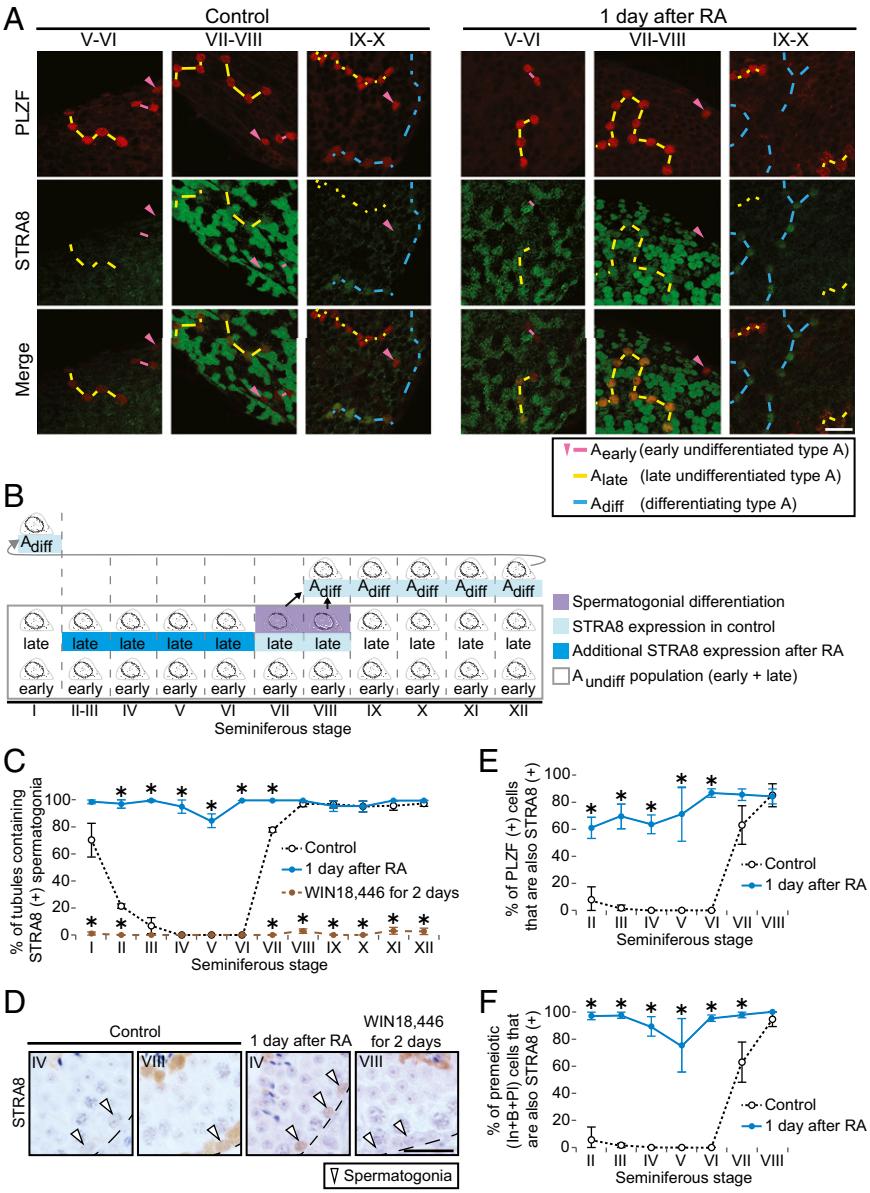

Fig. 4. STRA8 protein is normally present in late undifferentiated spermatogonia and can be precociously induced by injected RA. (*A*) Whole-mount immunostaining of intact wild-type testis tubules for PLZF (red) and STRA8 (green), in controls (*Left*) and 1 d after RA injection (*Right*). Arrowheads: isolated (single) spermatogonia. Dashed lines: putative interconnected chains of spermatogonia. Magenta labels: early undifferentiated type A spermatogonia (A_{early}). Yellow labels: late undifferentiated type A spermatogonia (A_{late}). Blue labels: differentiating type A spermatogonia (A_{diff}). (Scale bar, 30 μm.) (*B*) Diagram of STRA8 expression in type A spermatogonia, in controls (light blue) and 1 d after RA injection (light blue + dark blue). Diagram is based on observations in *A* and *C*. A_{undiff}, early, late, and A_{diff}: undifferentiated type A, early undifferentiated type A, late undifferentiated type A, and differentiating type A spermatogonia. (*C*) Percentage of testis tubule cross-sections containing STRA8-positive spermatogonia, in controls, 1 d after a single RA injection, and after 2 d of WIN18,446 treatment. Control data are duplicated from Fig. S1C. Error bars, mean ± SD *$P < 0.01$ (one-tailed Welch's *t* test). (*D*) Immunostaining for STRA8 on testis cross-sections in stages IV and VIII. Dashed lines: basal laminae. Arrowheads: spermatogonia. (Scale bar, 30 μm.) (*E* and *F*) Percentage of PLZF-positive cells (*E*) or PLZF-negative premeiotic cells (*F*) that are also positive for STRA8 in testis cross-sections, in controls or 1 d after RA injection. Premeiotic germ cells (ln+B+Pl): intermediate and type B spermatogonia and preleptotene spermatocytes. Error bars, mean ± SD *$P < 0.01$ (one-tailed Welch's *t* test).

Injected RA Induces Precocious Spermatogonial Differentiation. Because injected RA induced precocious STRA8 expression in stages II–VI, and STRA8 promotes spermatogonial differentiation, we hypothesized that RA would also induce spermatogonial differentiation in these stages. In the unperturbed testis, as a consequence of their differentiation in stages VII–VIII, spermatogonia express KIT protooncogene and enter mitotic S phase. They eventually develop into type B spermatogonia, then become preleptotene spermatocytes, and then initiate meiosis to become leptotene spermatocytes. We predicted that RA injection would cause undifferentiated spermatogonia to precociously begin this developmental progression.

We first confirmed that RA injection induced precocious KIT expression in spermatogonia. In control testis sections, KIT expression was absent in type A spermatogonia in stages II–VI and present in stages VII–VIII (Fig. S4 *E* and *G*) (7). As predicted, at 1 d after RA injection, KIT was strongly induced in stages II–VI. We next tested for precocious entry into S phase, using PLZF to identify undifferentiated and newly differentiating spermatogonia, and BrdU incorporation to assay for S phase (Fig. S4 *F* and *H*). Indeed, at 1 d after RA injection, many PLZF-positive spermatogonia in stages II–VIII incorporated BrdU, whereas in control testes BrdU incorporation did not begin until stage VIII (10, 38).

If injected RA had induced precocious spermatogonial differentiation, the spermatogonia should develop into type B spermatogonia, preleptotene spermatocytes, and leptotene spermatocytes after 7, 8.6, and 10.6 d, respectively (Figs. 1*B* and 5*A*) (11). Thus, we should see transient increases in these cell types. As predicted, at 7 d after RA injection, type B spermatogonia were present in an increased fraction of testis tubules, in a much broader range of stages (XII–VI) than in control testes (IV–VI) (Fig. 5 *B* and *C* and Fig. S5*A*). Preleptotene spermatocytes were similarly increased at 8.6 d after RA injection (in stages II–VIII, vs. VI–VIII in control testes) (Fig. 5 *D* and *E* and Fig. S5*B*); throughout these stages, most of the premeiotic cells in the tubule cross-sections were preleptotene spermatocytes (Fig. S5*D*). Finally, at 10.6 d after RA injection, leptotene spermatocytes were present in an increased fraction of tubules, throughout stages VI–X (vs. VIII–X in control testes) (Fig. 5 *F* and *G* and Fig. S5*C*). We confirmed our identification of leptotene spermatocytes throughout this broad range of stages by immunostaining for meiotic markers: γH2AX (phosphorylated H2A histone family member X, a marker of DNA double strand breaks)

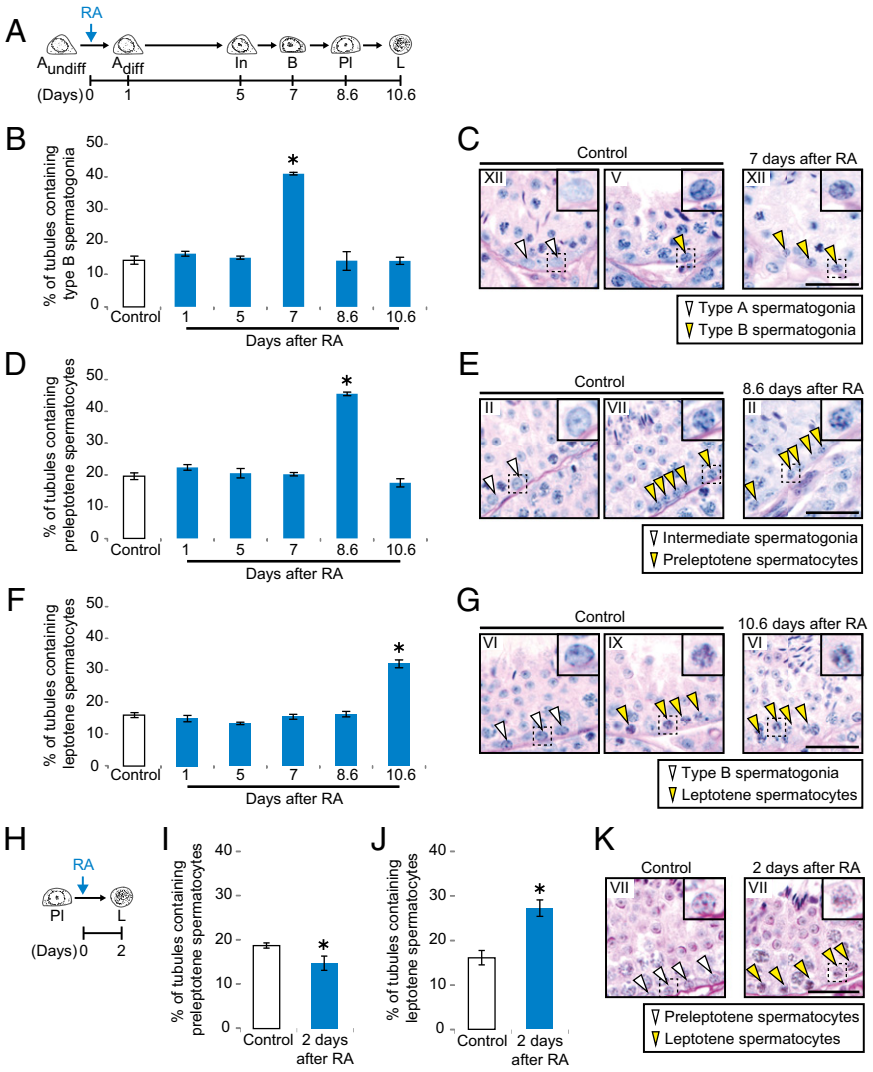

Fig. 5. Injected RA induces precocious spermatogonial differentiation and meiotic initiation. (*A*) Diagram of predicted germ-cell development after RA-induced spermatogonial differentiation. (*B*, *D*, and *F*) Percentage of tubules containing type B spermatogonia (*B*), preleptotene spermatocytes (*D*), or leptotene spermatocytes (*F*), in control or RA-injected testis cross-sections. Error bars, mean ± SD **P* < 0.01 compared with control (Dunnett's test). (*C*, *E*, and *G*) Control and RA-injected testis cross-sections, stained with hematoxylin and periodic acid-Schiff (He-PAS). Roman numerals indicate stages. Insets enlarge the boxed regions. Arrowheads in *C*: type A (white) and type B (yellow) spermatogonia. Arrowheads in *E*: intermediate spermatogonia (white) and preleptotene spermatocytes (yellow). Arrowheads in *G*: type B spermatogonia (white) and leptotene spermatocytes (yellow). (Scale bars, 30 μm.) (*H*) Diagram of predicted germ-cell development after RA-induced meiotic initiation. (*I* and *J*) Percentage of tubules containing preleptotene (*I*) or leptotene (*J*) spermatocytes, in control or RA-injected testis cross-sections. Error bars, mean ± SD **P* < 0.01 compared with control (Dunnett's test). (*K*) Control and RA-injected testis cross-sections, stained with He-PAS. Roman numerals indicate stages. Insets enlarge boxed regions. Arrowheads: preleptotene (white) and leptotene (yellow) spermatocytes. (Scale bars, 30 μm.)

(39) and SYCP3 (synaptonemal complex protein 3) (40). Indeed, at 10.6 d after RA injection, leptotene spermatocytes in stages VI–X were γH2AX- and SYCP3-positive (Fig. 6*A*). The stages at which type B spermatogonia, preleptotene spermatocytes, and leptotene spermatocytes appeared after RA injection were completely consistent with spermatogonial differentiation having occurred throughout stages II–VIII (Fig. S5 *E*–*G* and Table S2).

We conclude that injected RA induced precocious spermatogonial differentiation. The precociously differentiated spermatogonia then progressed into meiotic prophase, ahead of schedule. Spermatogonial differentiation was limited to stages II–VIII, whereas undifferentiated spermatogonia in stages IX–I were seemingly unaffected by RA.

Injected RA Induces Precocious Meiotic Initiation. Because injected RA induces precocious STRA8 expression in both premeiotic cells and undifferentiated spermatogonia, and STRA8 is required for meiotic initiation, we hypothesized that injected RA would also induce precocious meiotic initiation. In the unperturbed testis, germ cells initiate meiosis in late stage VII and stage VIII and then develop into leptotene spermatocytes 2 d later. Thus, we expect a transient increase in leptotene spermatocytes at 2 d after RA injection. Indeed, leptotene spermatocytes were present in an increased fraction of testis tubules, in a broader range of stages (VII–X) than in control testes (VIII–X). The percentage of tubules containing preleptotene spermatocytes was correspondingly decreased (Fig. 5 *H*–*K* and Fig. S5*H*). The precocious leptotene cells had normal meiotic γH2AX and SYCP3 expression patterns (Fig. 6*B*). To confirm that precocious meiotic initiation was a specific effect of RA–STRA8 signaling, we used WIN18,446 to chemically block RA synthesis and inhibit STRA8 expression (Fig. S5*I*). As expected, WIN18,446 prevented meiotic initiation in preleptotene spermatocytes (Fig. S5 *J* and *K*). We also confirmed that the precocious leptotene spermatocytes could progress normally through meiosis (Fig. S6 and *SI Results and Discussion*).

Our results show that premeiotic cells initiated meiosis precociously in response to injected RA and then progressed normally through meiosis, ahead of their usual schedule. However, precocious meiotic initiation occurred in fewer tubules than precocious spermatogonial differentiation (Fig. 5 *B* and *J*), strongly suggesting that the window of competence for meiotic initiation was narrower than that for spermatogonial differentiation. Based on the stages in which leptotene spermatocytes, zygotene spermatocytes, and meiotically dividing cells appeared after RA injection, we calculate that precocious meiotic initiation occurred in stage VI, and perhaps also in stages IV–V. This contrasts with precocious spermatogonial differentiation, which occurred throughout stages II–VI. Moreover, only premeiotic cells, not undifferentiated spermatogonia, were able to initiate

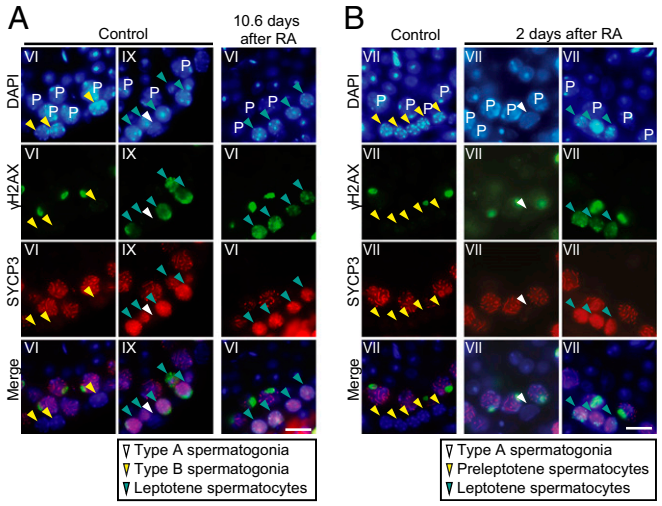

Fig. 6. Injected RA induces precocious expression of meiotic markers. (*A* and *B*) Immunostaining for γH2AX (green) and SYCP3 (red), with DAPI counterstain (blue), on control and RA-injected testis cross-sections. Roman numerals indicate stages. Arrowheads in *A*: type A spermatogonia (white), type B spermatogonia (yellow), and leptotene spermatocytes (green). Arrowheads in *B*: type A spermatogonia (white), preleptotene spermatocytes (yellow), and leptotene spermatocytes (green). P: pachytene spermatocytes. (Scale bars, 10 μm.)

meiosis directly in response to RA, as judged by the absence of γH2AX and SYCP3 signals in type A spermatogonia, 2 d after RA injection (Fig. 6*B*). Thus, the competencies of germ cells to interpret the RA–STRA8 signal are distinct between undifferentiated spermatogonia and premeiotic cells.

Competencies for Spermatogonial Differentiation and Meiotic Initiation Are Limited to Distinct Subsets of Germ Cells. We set out to verify these distinct competencies using more stringent criteria. In the unperturbed testis, the seminiferous cycle lasts 8.6 d (i.e., in a given tubule section, spermatogonial differentiation and meiotic initiation occur once every 8.6 d) (Fig. 1*B*). We administered successive RA injections, once per 8.6-d cycle (Fig. 7*A*). We then predicted when different germ-cell types should appear, based on our findings that competence for spermatogonial differentiation was limited to stages II–VIII, that competence for meiotic initiation was limited to a subset of these stages, and that germ cells developed normally after precocious spermatogonial differentiation/meiotic initiation.

Competence for meiotic initiation. We first predicted that premeiotic cells in stages VI–VIII (and possibly also in stages IV/V), having initiated meiosis, would develop into step 7–8 spermatids after two 8.6-d intervals of RA injection (2 × 8.6 d) (Fig. 1*B*). Indeed, an increased percentage of tubules contained step 7–8 spermatids; step 6 spermatids were correspondingly depleted (Fig. S7*A*). Step 2–5 spermatids were virtually unchanged, demonstrating that meiotic initiation occurred specifically in stages VI–VIII, not in stages IV–V.

Competence for spermatogonial differentiation. We next predicted that spermatogonia in stages II–VIII, having differentiated, would develop into step 7–8 spermatids after 3 × 8.6 d of RA injection, then develop into spermatozoa after 4 × 8.6 d, and finally be released into the tubule lumen (Fig. 1*B*). Indeed, we saw increases in step 7–8 spermatids and spermatozoa after 3 × 8.6 d and 4 × 8.6 d, respectively (Fig. 7 *B* and *C* and Fig. S7*A*). Successive RA injections were able to repeatedly induce spermatogonial differentiation; at 4 × 8.6 d, spermatozoa combined with younger RA-induced generations of germ cells to produce an excess of stage VII/VIII germ-cell associations, with a corresponding depletion of stages II–VI (Fig. 7*B*). Finally, after 4 × 8.6 plus 2 d of RA injection (36.4 d total), an increased percentage of tubules had released their spermatozoa (Fig. S7 *B–D*). All these results are entirely consistent with competence for spermatogonial differentiation being limited to stages II–VIII.

Competence for neither. Finally, because germ cells in stages IX–I are competent for neither spermatogonial differentiation nor meiotic initiation, they should be unaffected by successive RA

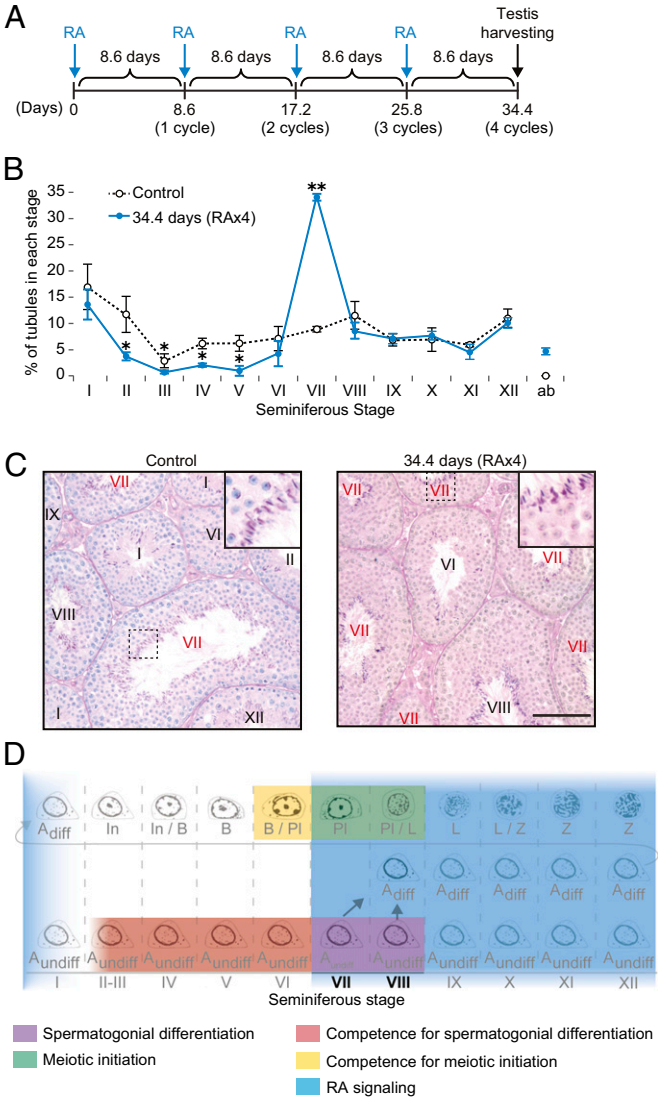

Fig. 7. Periodic RA–STRA8 signaling intersects with periodic germ-cell competencies to regulate spermatogenesis. (*A*) Diagram of four successive RA injections. Testes were harvested 34.4 d after the first RA injection. (*B*) Percentage of tubules in each stage of seminiferous cycle, in controls and after four RA injections. Abnormal germ-cell associations indicated by "ab"; all other germ-cell associations are fully normal. Error bars, mean ± SD $*P < 0.05$, $**P < 0.01$ (two-tailed Welch's *t* test). (*C*) Testis cross-sections, stained with He-PAS, in controls (*Left*) or after four RA injections (*Right*). Cross-sections with the highest frequency of stage VII tubules (red) were selected. Stage VII tubules contain spermatozoa, clustered around the tubule lumen. Roman numerals indicate stages. Insets enlarge boxed regions. (Scale bar, 100 μm.) (*D*) Model: Periodic RA–STRA8 signaling and periodic germ-cell competencies regulate spermatogonial differentiation and meiotic initiation. Red: competence for spermatogonial differentiation. Yellow: competence for meiotic initiation. Blue: stages in which we infer RA signaling is active. Competence for spermatogonial differentiation intersects with RA signaling to induce spermatogonial differentiation (purple). Competence for meiotic initiation intersects with RA signaling to induce meiotic initiation (green).

injections. Indeed, after 4 × 8.6 d of RA injections, the frequency of stage IX–I tubules was the same as in controls (Fig. 7*B*).

We found that, when germ cells are provided with RA, competence to undergo spermatogonial differentiation is strictly limited to stages II–VIII, whereas competence to undergo meiotic initiation is strictly limited to stages VI–VIII. The accuracy of our predictions, over long time scales, demonstrated that these windows of competence are precise. Furthermore, germ cells were able to develop at their normal pace after precocious spermatogonial differentiation/meiotic initiation. This development occurred even when germ cells were outside of their usual cell associations. Injected RA is thus able to accelerate spermatogenesis. Finally, we note that successive RA injections, combined with intrinsic germ-cell competencies, repeatedly induced spermatogonial differentiation; four successive injections were thus able to reestablish normal stage VII/VIII germ-cell associations (Fig. 7 *B* and *C*). We conclude that spermatogonial differentiation and meiotic initiation are regulated by a shared RA–STRA8 signal intersecting with two distinct germ-cell competencies (Fig. 7*D*).

Discussion

RA–STRA8 Signaling Coordinates Spermatogonial Differentiation and Meiotic Initiation. Spermatogenesis in rodents is elaborately organized, with multiple generations of germ cells developing in stereotypical cell associations. This organization was first reported in 1888 (15) and by the 1950s had been comprehensively described (13, 33, 41). To understand spermatogenesis, we must systematically perturb its organization. Here, we used two complementary perturbations, genetic ablation of *Stra8* function and chemical manipulation of RA levels, to probe the coordination of two key transitions: spermatogonial differentiation and meiotic initiation.

We report that RA–STRA8 signaling plays an instructive role in both spermatogonial differentiation and meiotic initiation, inducing these transitions to occur together. Specifically, we provide the first functional evidence to our knowledge that STRA8, an RA target gene, promotes spermatogonial differentiation (as well as being required for meiotic initiation) (24, 25). In the absence of *Stra8*, spermatogonial differentiation was impaired: Undifferentiated spermatogonia began to accumulate as early as p10, ultimately giving rise to massive accumulations of type A spermatogonia in aged testes. These findings show that RA acts instructively at spermatogonial differentiation, by altering gene expression in spermatogonia. Genetic ablation of *Stra8* did not completely block spermatogonial differentiation, indicating that RA must act through additional targets at this transition. Additional targets could be activated either directly by RARs in spermatogonia, or indirectly, by the action of RA on the supporting somatic (Sertoli) cells of testis. Indeed, indirect RA signaling, via RARα in Sertoli cells, is critical for the first round of spermatogonial differentiation (42). We also report that, in wild-type mice, RA injection induced precocious spermatogonial differentiation and meiotic initiation. We infer that, in the unperturbed wild-type testis, a single pulse of RA signaling drives STRA8 expression in both undifferentiated spermatogonia and premeiotic spermatocytes and induces two distinct, cell-type-specific responses. This shared RA–STRA8 signal helps to ensure that spermatogonial differentiation and meiotic initiation occur at the same time and place (Fig. 7*D*).

Evidence of Elevated RA Concentration in Stages VII–XII/I. In any given tubule cross-section, spermatogonial differentiation and meiotic initiation occur periodically, once every 8.6 d. Sugimoto et al. (43) and Hogarth et al. (44) have hypothesized that RA concentration also varies periodically over the course of this 8.6-d cycle. This hypothesis is supported by expression data, functional studies, and direct measurements of RA levels (34, 43, 45, 46). However, the pattern of RA periodicity was previously unclear. Hogarth et al. (34, 44) suggested a sharp RA peak in stages VIII–IX. In contrast, based on expression patterns of RA-responsive genes and the functional consequences of inhibiting RA signaling, Hasegawa and Saga (45) suggested that RA levels rise in stage VII and remain high through stage XII.

Our data support the latter model, of a prolonged elevation of RA levels (Fig. 7*D*). We and others (35) have demonstrated that, in the unperturbed testis, STRA8 is periodically expressed and is present for the majority of the seminiferous cycle. Specifically, we show that STRA8 protein is present in spermatogonia in stages VII–XII/I and absent in II–VI. Furthermore, we show that, at the level of the tubule cross-section, spermatogonial STRA8 expression marks the presence of RA: When we increased RA levels by injecting RA or decreased them by injecting WIN18,446, STRA8 expression was immediately induced or repressed in all seminiferous stages (Fig. 4*C*). We thus agree with and extend the model of Hasegawa and Saga (45): In the unperturbed testis, RA levels rise in stage VII, rapidly inducing STRA8 and then inducing spermatogonial differentiation and meiotic initiation. RA levels remain high until stages XII/I. This model of a long RA–STRA8 pulse is consistent with additional published data. First, the enzyme *Aldh1a2,* which increases RA levels, is strongly expressed in stages VII–XII, whereas the enzymes *Lrat* and *Adfp*, which reduce RA levels, are expressed in stages I–VI/VII (43, 46). Second, although measured RA levels seem to peak in stages VIII–IX, they remain elevated for an extended period (2–4 d in pubertal animals, and through stage XII in adults) (34). Despite these persistently elevated RA levels, neither spermatogonial differentiation nor meiotic initiation recurs in stages IX–I. As we will now discuss, germ cells at these later stages lack competence for these transitions.

Undifferentiated Spermatogonia and Premeiotic Cells Have Different Competencies to Respond to RA–STRA8 Signaling. By examining responses to exogenous RA, we provide functional evidence that germ cells have periodic, stage-limited competencies to undergo spermatogonial differentiation and meiotic initiation. These competencies intersect with instructive, periodic RA–STRA8 signaling. Specifically, undifferentiated spermatogonia are competent for spermatogonial differentiation in stages II–VIII, and premeiotic cells are competent for meiotic initiation in stages VI–VIII (Fig. 7*D*). Competencies for both transitions begin while RA levels are low, so that the germ cells respond as soon as RA levels rise. Competencies for both transitions end simultaneously, while RA levels are still high. Thus, germ-cell competencies and high RA levels intersect briefly, causing spermatogonial differentiation and meiotic initiation to occur at the same time and place (in stages VII–VIII).

We also conclude that undifferentiated spermatogonia and premeiotic cells enact different molecular and cellular programs in response to RA–STRA8 signaling. In response to injected RA, only preleptotene spermatocytes (and possibly late type B spermatogonia, the immediate precursors of preleptotene spermatocytes) began to express meiotic markers such as SYCP3 and γH2AX. Undifferentiated spermatogonia were not competent to initiate meiosis directly. Instead, in response to injected RA, most late undifferentiated spermatogonia began a program of spermatogonial differentiation, followed by six mitotic cell divisions. The early undifferentiated spermatogonia and a fraction of the late undifferentiated spermatogonia were seemingly unaffected by RA; they did not express STRA8 and did not differentiate. We believe that these undifferentiated spermatogonia are able to self-renew and proliferate even in the presence of RA, preventing the pool of undifferentiated spermatogonia from becoming depleted. Indeed, a normal complement of germ cells remained after repeated RA injections, indicating that injected RA did not eliminate the pool of undifferentiated spermatogonia (which includes the spermatogonial stem cells). Thus, distinct germ-cell competencies enable a single RA signal to induce both

spermatogonial differentiation and meiotic initiation and ensure that a subset of spermatogonia are able to self-renew and proliferate despite exposure to the RA signal.

We do not yet know the molecular mechanism behind the stage- and cell-type-specific competencies to differentiate in response to RA. These competencies cannot simply be explained by RAR expression, because the RARs do not have precise stage-specific expression patterns. For instance, RARγ expression can be observed in all stages of the seminiferous cycle (21, 46). The competencies must therefore result from other aspects of germ-cell state. We note that competence for spermatogonial differentiation is closely correlated with proliferative activity. Specifically, undifferentiated spermatogonia in stages II–VIII, which are competent for differentiation, are arrested in the G0/G1 phase of the cell cycle, whereas undifferentiated spermatogonia in stages IX–I are actively proliferating (10, 38). Further studies are needed to identify the mechanisms by which competencies to undergo spermatogonial differentiation, and then meiotic initiation, are achieved.

The critical role for intrinsic germ-cell competence during spermatogenesis is in some respects analogous to its role of competence during oogenesis. In adult ovaries, immature oocytes are arrested at the diplotene stage of meiotic prophase. Some of these arrested oocytes grow and acquire intrinsic competence to resume meiosis and then acquire competence to mature (i.e., to progress to metaphase II arrest) (47, 48). These serially acquired competencies intersect with extrinsic, hormonal signals. We suggest that, in both oogenesis and spermatogenesis, properly timed differentiation depends on the intersection of extrinsic chemical cues and intrinsic competence.

RA–STRA8 Signaling Can Both Perturb and Reestablish the Complex Organization of the Testis. We find that injected RA can induce spermatogonial differentiation and meiotic initiation to occur precociously and ectopically, outside of their normal context. In the unperturbed testis, these two transitions occur together at stages VII/VIII, but, following a single RA injection, they occurred in different stages, with spermatogonial differentiation as early as stage II and meiotic initiation as early as stage VI. Then, when provided with RA at 8.6-d intervals, these precociously advancing germ cells were able to complete meiosis and develop into spermatozoa, ahead of schedule. This developmental flexibility is surprising, given the seemingly rigid organization of spermatogenesis (11). In the unperturbed testis, multiple generations of germ cells occur together in stereotypical associations; these associations are conserved across mammals and, before this study, had proven difficult to chemically disrupt (43, 49, 50). Nevertheless, when provided with RA, germ cells proceeded through spermatogenesis, outside of their usual environs, with no apparent guidance from the neighboring germ cells.

Why is spermatogenesis so precisely organized, if the stereotypical associations are not required for germ-cell development? We posit that this precise organization is in part a by-product of RA–STRA8 signaling (and germ-cell competencies): Cooccurrence of spermatogonial differentiation and meiotic initiation nucleates the stereotypical germ-cell associations. In support of this idea, when we administered successive RA injections at 8.6-d intervals, to repeatedly drive precocious spermatogonial differentiation and meiotic initiation, we were able to perturb and reestablish the characteristic germ-cell associations in vivo. The stereotypical associations, established by RA–STRA8 signaling, may ensure the efficiency of spermatogenesis.

We conclude that a simple regulatory mechanism helps to explain the testis's extraordinary capacity for proliferation and differentiation. Periodic RA signaling repeatedly induces spermatogonial differentiation and meiotic initiation, driving germ cells toward becoming highly specialized haploid spermatozoa. Meanwhile, distinct germ-cell competencies enforce that every spermatogonium undergoes programmed amplifying divisions before initiating meiosis, guaranteeing a prodigious output of spermatozoa. Moreover, a fraction of spermatogonia undergo neither spermatogonial differentiation nor meiotic initiation in response to RA, ensuring that a reservoir of undifferentiated spermatogonia is maintained throughout the animal's reproductive lifetime. This basic understanding of the organization of spermatogenesis, derived from genetic and chemical perturbations, will facilitate future studies of germ-cell development, RA-driven differentiation, and cell competence, both in vivo and in vitro.

Materials and Methods

Mice. Three types of mice were used: wild-type (C57BL/6NtacfBR), *Stra8*-deficient (extensively back-crossed to C57BL/6) (26, 27), and *Dmc1*-deficient (B6.Cg-Dmc1^{tm1Jcs}/JcsJ) (51). See *SI Materials and Methods* for strain and genotyping details. Unless otherwise noted, experiments were performed on 6- to 8-wk-old male mice, fed a regular (vitamin A-sufficient) diet. All experiments involving mice were approved by the Committee on Animal Care at the Massachusetts Institute of Technology.

Statistics. Data are represented as mean ± SD of three biological replicates. To compare two groups, Welch's *t* test (one- or two-tailed as indicated) or the Mann–Whitney *U* test were used. To compare three or more groups, one-way ANOVA with the Tukey–Kramer post hoc test was used. To compare multiple experimental groups with a control group, one-way ANOVA with Dunnett's post hoc test was used. To compare distributions, the Kolmogorov–Smirnov test was used. When performing genome-wide analysis of mRNA-Seq data, the Benjamini–Hochberg procedure was used to control the false discovery rate.

mRNA-Seq Sample Preparation. Testes were stripped of the tunica albuginea, placed in TRIzol (Invitrogen), homogenized, and stored at −20 °C. Total RNAs were prepared according to the manufacturer's protocol. Total RNAs were then DNase-treated using DNA Free Turbo (Ambion). Libraries were prepared using the Illumina mRNA-Seq Sample Preparation Kit according to the manufacturer's protocol. Libraries were validated with an Agilent Bioanalyzer. Libraries were diluted to 10 pM and applied to an Illumina flow cell using the Illumina Cluster Station. The Illumina Genome Analyzer II platform was used to sequence 36-mers (single end) from the mRNA-Seq libraries.

mRNA-Seq and Microarray Data Analysis. For mRNA-Seq data, reads were aligned to the mouse genome using TopHat (52). Analysis was performed using edgeR (53), Cufflinks (54), and custom R scripts. Microarray data were normalized with the GCRMA package from Bioconductor, and replicates were averaged using limma (55). Comparison mRNA-Seq and microarray datasets were downloaded from National Center for Biotechnology Information GEO and Sequence Read Archive (SRA). See *SI Materials and Methods* for details on mRNA-Seq and microarray data processing and comparison.

Histology. Testes were fixed overnight in Bouin's solution, embedded in paraffin, sectioned, and stained with hematoxylin and eosin, or with hematoxylin and periodic acid-Schiff (PAS). All sections were examined using a light microscope. Germ-cell types were identified by their location, nuclear size, and chromatin pattern (11). See *SI Materials and Methods* for details on identification of the stages of the seminiferous cycle.

Chemical Treatments. For RA injection experiments, mice received i.p. injections of 100 μL of 7.5 mg/mL all-*trans* RA (Sigma-Aldrich) in 16% (vol/vol) DMSO–H_2O. For BrdU incorporation experiments, mice received i.p. injections of 10 μL/g body weight of 10 mg/mL BrdU (Sigma-Aldrich) in PBS, 4 h before they were killed. For WIN18,446 injection experiments, mice received i.p. injections of 100 μL of 20 mg/mL WIN18,446 (sc-295819A; Santa Cruz Biotechnology) in 16% DMSO–H_2O; mice were dosed at intervals of 12 h for a total of 2 or 4 d.

Immunostaining on Testis Sections. Testes were fixed overnight in Bouin's solution or 4% (wt/vol) paraformaldehyde, embedded in paraffin, and sectioned at 5-μm thickness. Slides were dewaxed, rehydrated, and heated in 10 mM sodium citrate buffer (pH 6.0). Sections were then blocked, incubated with the primary antibody, washed with PBS, incubated with the secondary antibody, and washed with PBS. Detection was fluorescent or

colorimetric. Antibodies and incubation conditions are provided in *SI Materials and Methods* and in Table S3.

Immunostaining on Intact Testis Tubules. Testes were stripped of the tunica albuginea, dispersed in PBS, fixed overnight in 4% paraformaldehyde at 4 °C, and washed with PBS. Testes were blocked with 2.5% (vol/vol) donkey serum, incubated with the primary antibody, washed with PBS, incubated with the secondary antibody, and washed with PBS. Finally, seminiferous tubules were dissected from testes and mounted with SlowFade Gold antifade reagent with DAPI (S36939; Life Technologies). Antibodies and incubation conditions are provided in *SI Materials and Methods*.

ACKNOWLEDGMENTS. We thank H. Skaletsky for statistical advice; M. E. Gill for helpful discussions; and D. W. Bellott, T. Bhattacharyya, M. Carmell, J. Hughes, M. Kojima, B. Lesch, S. Naqvi, P. Nicholls, T. Shibue, S. Soh, and L. Teitz for critical reading of the manuscript. This work was supported by the Howard Hughes Medical Institute and by NIH Pre-Doctoral Training Grant T32GM007287.

1. Nakagawa T, Nabeshima Y, Yoshida S (2007) Functional identification of the actual and potential stem cell compartments in mouse spermatogenesis. *Dev Cell* 12(2): 195–206.
2. Tegelenbosch RA, de Rooij DG (1993) A quantitative study of spermatogonial multiplication and stem cell renewal in the C3H/101 F1 hybrid mouse. *Mutat Res* 290(2): 193–200.
3. Brinster RL, Zimmermann JW (1994) Spermatogenesis following male germ-cell transplantation. *Proc Natl Acad Sci USA* 91(24):11298–11302.
4. Shinohara T, Orwig KE, Avarbock MR, Brinster RL (2000) Spermatogonial stem cell enrichment by multiparameter selection of mouse testis cells. *Proc Natl Acad Sci USA* 97(15):8346–8351.
5. Zheng K, Wu X, Kaestner KH, Wang PJ (2009) The pluripotency factor LIN28 marks undifferentiated spermatogonia in mouse. *BMC Dev Biol* 9:38.
6. Pesce M, Wang X, Wolgemuth DJ, Schöler H (1998) Differential expression of the Oct-4 transcription factor during mouse germ cell differentiation. *Mech Dev* 71(1-2):89–98.
7. Tokuda M, Kadokawa Y, Kurahashi H, Marunouchi T (2007) CDH1 is a specific marker for undifferentiated spermatogonia in mouse testes. *Biol Reprod* 76(1):130–141.
8. Kanatsu-Shinohara M, et al. (2004) Generation of pluripotent stem cells from neonatal mouse testis. *Cell* 119(7):1001–1012.
9. Buaas FW, et al. (2004) Plzf is required in adult male germ cells for stem cell self-renewal. *Nat Genet* 36(6):647–652.
10. Lok D, de Rooij DG (1983) Spermatogonial multiplication in the Chinese hamster. III. Labelling indices of undifferentiated spermatogonia throughout the cycle of the seminiferous epithelium. *Cell Tissue Kinet* 16(1):31–40.
11. Russell LD, Ettlin RA, Sinha Hikim AP, Clegg ED (1990) *Histological and Histopathological Evaluation of the Testis* (Cache River, Clearwater, FL).
12. Huckins C (1971) The spermatogonial stem cell population in adult rats. I. Their morphology, proliferation and maturation. *Anat Rec* 169(3):533–557.
13. Leblond CP, Clermont Y (1952) Spermiogenesis of rat, mouse, hamster and guinea pig as revealed by the periodic acid-fuchsin sulfurous acid technique. *Am J Anat* 90(2): 167–215.
14. Lok D, Weenk D, De Rooij DG (1982) Morphology, proliferation, and differentiation of undifferentiated spermatogonia in the Chinese hamster and the ram. *Anat Rec* 203(1):83–99.
15. von Ebner V (1888) Zur spermatogenese bei den säugethieren. *Arch f Mikr Anat* 31(1): 236–292. German.
16. Van Pelt AMM, De Rooij DG (1990) The origin of the synchronization of the seminiferous epithelium in vitamin A-deficient rats after vitamin A replacement. *Biol Reprod* 42(4):677–682.
17. van Pelt AMM, de Rooij DG (1990) Synchronization of the seminiferous epithelium after vitamin A replacement in vitamin A-deficient mice. *Biol Reprod* 43(3):363–367.
18. van Pelt AMM, de Rooij DG (1991) Retinoic acid is able to reinitiate spermatogenesis in vitamin A-deficient rats and high replicate doses support the full development of spermatogenic cells. *Endocrinology* 128(2):697–704.
19. Morales C, Griswold MD (1987) Retinol-induced stage synchronization in seminiferous tubules of the rat. *Endocrinology* 121(1):432–434.
20. Baleato RM, Aitken RJ, Roman SD (2005) Vitamin A regulation of BMP4 expression in the male germ line. *Dev Biol* 286(1):78–90.
21. Gely-Pernot A, et al. (2012) Spermatogonia differentiation requires retinoic acid receptor γ. *Endocrinology* 153(1):438–449.
22. Bowles J, et al. (2006) Retinoid signaling determines germ cell fate in mice. *Science* 312(5773):596–600.
23. Koubova J, et al. (2006) Retinoic acid regulates sex-specific timing of meiotic initiation in mice. *Proc Natl Acad Sci USA* 103(8):2474–2479.
24. Anderson EL, et al. (2008) Stra8 and its inducer, retinoic acid, regulate meiotic initiation in both spermatogenesis and oogenesis in mice. *Proc Natl Acad Sci USA* 105(39): 14976–14980.
25. Baltus AE, et al. (2006) In germ cells of mouse embryonic ovaries, the decision to enter meiosis precedes premeiotic DNA replication. *Nat Genet* 38(12):1430–1434.
26. Oulad-Abdelghani M, et al. (1996) Characterization of a premeiotic germ cell-specific cytoplasmic protein encoded by Stra8, a novel retinoic acid-responsive gene. *J Cell Biol* 135(2):469–477.
27. Zhou Q, et al. (2008) Expression of stimulated by retinoic acid gene 8 (Stra8) in spermatogenic cells induced by retinoic acid: An in vivo study in vitamin A-sufficient postnatal murine testes. *Biol Reprod* 79(1):35–42.
28. Zhou Q, et al. (2008) Expression of stimulated by retinoic acid gene 8 (Stra8) and maturation of murine gonocytes and spermatogonia induced by retinoic acid in vitro. *Biol Reprod* 78(3):537–545.
29. Wang PJ, McCarrey JR, Yang F, Page DC (2001) An abundance of X-linked genes expressed in spermatogonia. *Nat Genet* 27(4):422–426.
30. Namekawa SH, et al. (2006) Postmeiotic sex chromatin in the male germline of mice. *Curr Biol* 16(7):660–667.
31. Costoya JA, et al. (2004) Essential role of Plzf in maintenance of spermatogonial stem cells. *Nat Genet* 36(6):653–659.
32. Nakagawa T, Sharma M, Nabeshima Y, Braun RE, Yoshida S (2010) Functional hierarchy and reversibility within the murine spermatogenic stem cell compartment. *Science* 328(5974):62–67.
33. Oakberg EF (1956) A description of spermiogenesis in the mouse and its use in analysis of the cycle of the seminiferous epithelium and germ cell renewal. *Am J Anat* 99(3): 391–413.
34. Hogarth CA, et al. (2015) Processive pulses of retinoic acid propel asynchronous and continuous murine sperm production. *Biol Reprod* 92(2):37.
35. Mark M, Teletin M, Vernet N, Ghyselinck NB (2015) Role of retinoic acid receptor (RAR) signaling in post-natal male germ cell differentiation. *Biochim Biophys Acta* 1849(2):84–93.
36. Amory JK, et al. (2011) Suppression of spermatogenesis by bisdichloroacetyldiamines is mediated by inhibition of testicular retinoic acid biosynthesis. *J Androl* 32(1): 111–119.
37. Hogarth CA, et al. (2011) Suppression of Stra8 expression in the mouse gonad by WIN 18,446. *Biol Reprod* 84(5):957–965.
38. Oakberg EF (1971) Spermatogonial stem-cell renewal in the mouse. *Anat Rec* 169(3): 515–531.
39. Rogakou EP, Pilch DR, Orr AH, Ivanova VS, Bonner WM (1998) DNA double-stranded breaks induce histone H2AX phosphorylation on serine 139. *J Biol Chem* 273(10): 5858–5868.
40. Yuan L, et al. (2000) The murine SCP3 gene is required for synaptonemal complex assembly, chromosome synapsis, and male fertility. *Mol Cell* 5(1):73–83.
41. Oakberg EF (1956) Duration of spermatogenesis in the mouse and timing of stages of the cycle of the seminiferous epithelium. *Am J Anat* 99(3):507–516.
42. Raverdeau M, et al. (2012) Retinoic acid induces Sertoli cell paracrine signals for spermatogonia differentiation but cell autonomously drives spermatocyte meiosis. *Proc Natl Acad Sci USA* 109(41):16582–16587.
43. Sugimoto R, Nabeshima Y, Yoshida S (2012) Retinoic acid metabolism links the periodical differentiation of germ cells with the cycle of Sertoli cells in mouse seminiferous epithelium. *Mech Dev* 128(11-12):610–624.
44. Hogarth CA, et al. (2013) Turning a spermatogenic wave into a tsunami: Synchronizing murine spermatogenesis using WIN 18,446. *Biol Reprod* 88(2):40.
45. Hasegawa K, Saga Y (2012) Retinoic acid signaling in Sertoli cells regulates organization of the blood-testis barrier through cyclical changes in gene expression. *Development* 139(23):4347–4355.
46. Vernet N, et al. (2006) Retinoic acid metabolism and signaling pathways in the adult and developing mouse testis. *Endocrinology* 147(1):96–110.
47. Mehlmann LM (2005) Stops and starts in mammalian oocytes: Recent advances in understanding the regulation of meiotic arrest and oocyte maturation. *Reproduction* 130(6):791–799.
48. Sorensen RA, Wassarman PM (1976) Relationship between growth and meiotic maturation of the mouse oocyte. *Dev Biol* 50(2):531–536.
49. Meistrich ML (1986) Critical components of testicular function and sensitivity to disruption. *Biol Reprod* 34(1):17–28.
50. Snyder EM, Small C, Griswold MD (2010) Retinoic acid availability drives the asynchronous initiation of spermatogonial differentiation in the mouse. *Biol Reprod* 83(5):783–790.
51. Pittman DL, et al. (1998) Meiotic prophase arrest with failure of chromosome synapsis in mice deficient for Dmc1, a germline-specific RecA homolog. *Mol Cell* 1(5):697–705.
52. Trapnell C, Pachter L, Salzberg SL (2009) TopHat: Discovering splice junctions with RNA-Seq. *Bioinformatics* 25(9):1105–1111.
53. Robinson MD, McCarthy DJ, Smyth GK (2010) edgeR: A Bioconductor package for differential expression analysis of digital gene expression data. *Bioinformatics* 26(1): 139–140.
54. Trapnell C, et al. (2010) Transcript assembly and quantification by RNA-Seq reveals unannotated transcripts and isoform switching during cell differentiation. *Nat Biotechnol* 28(5):511–515.
55. Smyth GK (2005) limma: Linear models for microarray data. *Bioinformatics and Computational Biology Solutions Using R and Bioconductor*, eds Gentleman R, Carey VJ, Huber W, Irizarry RA, Dudoit S (Springer, New York), pp 397–420.

OPEN ACCESS Freely available online

PLOS ONE

An Integrative Omics Strategy to Assess the Germ Cell Secretome and to Decipher Sertoli-Germ Cell Crosstalk in the Mammalian Testis

Frédéric Chalmel[1]*[9], Emmanuelle Com[2][9], Régis Lavigne[2], Nolwen Hernio[2], Ana-Paula Teixeira-Gomes[3,4], Jean-Louis Dacheux[5], Charles Pineau[2]*

1 IRSET, Inserm U1085, Campus de Beaulieu, Rennes, France, **2** Proteomics Core Facility Biogenouest, Inserm U1085 IRSET, Campus de Beaulieu, Rennes, France, **3** INRA UMR 1282, Infectiologie et Santé Publique, Nouzilly, France, **4** INRA Plate-forme d'Analyse Intégrative des Biomolécules (PAIB[2]), Nouzilly, France, **5** UMR 85 INRA-CNRS, Nouzilly, France

Abstract

Mammalian spermatogenesis, which takes place in complex testicular structures called seminiferous tubules, is a highly specialized process controlled by the integration of juxtacrine, paracrine and endocrine information. Within the seminiferous tubules, the germ cells and Sertoli cells are surrounded by testicular fluid (TF), which probably contains most of the secreted proteins involved in crosstalk between these cells. It has already been established that germ cells can modulate somatic Sertoli cell function through the secretion of diffusible factors. We studied the germ cell secretome, which was previously considered inaccessible, by analyzing the TF collected by microsurgery in an "integrative omics" strategy combining proteomics, transcriptomics, genomics and interactomics data. This approach identified a set of proteins preferentially secreted by Sertoli cells or germ cells. An interaction network analysis revealed complex, interlaced cell-cell dialog between the secretome and membranome of seminiferous cells, mediated via the TF. We then focused on germ cell-secreted candidate proteins, and we identified several potential interacting partners located on the surface of Sertoli cells. Two interactions, APOH/CDC42 and APP/NGFR, were validated *in situ*, in a proximity ligation assay (PLA). Our results provide new insight into the crosstalk between germ cells and Sertoli cells occurring during spermatogenesis. Our findings also demonstrate that this "integrative omics" strategy is powerful enough for data mining and highlighting meaningful cell-cell communication events between different types of cells in a complex tissue, via a biological fluid. This integrative strategy could be applied more widely, to gain access to secretomes that have proved difficult to study whilst avoiding the limitations of *in vitro* culture.

Citation: Chalmel F, Com E, Lavigne R, Hernio N, Teixeira-Gomes A-P, et al. (2014) An Integrative Omics Strategy to Assess the Germ Cell Secretome and to Decipher Sertoli-Germ Cell Crosstalk in the Mammalian Testis. PLoS ONE 9(8): e104418. doi:10.1371/journal.pone.0104418

Editor: Wei Yan, University of Nevada School of Medicine, United States of America

Received March 28, 2014; **Accepted** July 8, 2014; **Published** August 11, 2014

Data Availability: The authors confirm that all data underlying the findings are fully available without restriction. All data are available from the PRIDE Proteomics Identifications database (http://www.ebi.ac.uk/pride) under the project names "Proteomic characterization of ram testicular fluid" and "Proteomic characterization of rat testicular fluid" (accession number: 31052-31111).

Funding: This work was supported by Biogenouest and Infrastructures en Biologie Santé et Agronomie (IBiSA), European Regional Development Fund and Conseil Régional de Bretagne grants. The funders had no role in study design, data collection and analysis, decision to publish, or preparation of the manuscript.

Competing Interests: The authors have declared that no competing interests exist.

* Email: charles.pineau@inserm.fr (CP); frederic.chalmel@inserm.fr (FC)

[9] These authors contributed equally to this work.

Background

Mammalian spermatogenesis, which takes place within the seminiferous tubules, is a multistep process conserved between species and playing a crucial role in the transmission of genetic heritage. Spermatogenesis can be split into three phases on the basis of anatomical and biochemical features: a proliferative or mitotic phase, in which the primitive germ cells – spermatogonia – renew themselves and undergo a series of mitotic divisions; the meiotic phase, in which the diploid spermatocytes undergo two consecutive divisions to produce haploid spermatids; and spermiogenesis, in which the spermatids develop into spermatozoa [1].

This unique process is controlled by juxtacrine, paracrine and endocrine factor signals, and is conditioned by the successive activation and/or repression of thousands of genes and proteins, including many testis-specific isoforms [for reviews, see [2–7]. All these features make the testis one of the most complex organs in the body [3] and this complex physiological structure creates particular difficulties for studies of testis organization, function and regulation. Studies of the interactions between Sertoli and germ cells are challenging, due to the anatomical complexity and probable interdependence of these cells.

Sertoli and germ cells probably communicate through a unique set of structural devices and functional interactions [2,8]. Sertoli cells were first described in 1865 [9] and are known to have nursing properties. They supply the germ cells, at all stages of development, with the factors they need for their division, differentiation and metabolism. They are also thought to help germ cells to synchronize their development and to help maintain the wave of spermatogenesis [for a review, see [3]]. Conversely, germ cells have been shown to regulate Sertoli cell function, in

both *in vivo* and *in vitro* studies. Since the late 1980s, the influence of germ cells has been known to be exerted through cell-cell contacts, via cytoplasmic structures allowing the transfer of germ cell materials [for a review see [3]] and the secretion of diffusible, proteinaceous factors [10–13]. However, differentiated germ cells have proved impossible to maintain *in vitro*, making it very difficult to study their secretome. For this reason, the role of these cells in spermatogenesis control has been largely neglected since it first emerged in the early 1990s [for a review see [3]].

The absence of such an "experimental testing ground" makes genome-wide "omics" approaches even more important. Significant progress has been made in the large-scale analysis of high-throughput data greatly increasing our knowledge of spermatogenesis, by making it possible to identify hundreds of genes displaying spatial and temporal regulation during the testicular ontogenesis essential for the differentiation of male gametes [for reviews, see [14–16]]. Our understanding of normal and pathological spermatogenesis has been greatly increased by the use of transcriptomics (microarrays and, more recently, RNA-sequencing technologies) and proteomics (differential and shotgun technologies) [for review see, [17–20]]. Nevertheless, with few exceptions [18,20–23], very little effort has been made to combine the resulting data in a cross-/multispecies integrative "omics" approach, to address specific biological questions relating to spermatogenesis.

The two compartments of the testis are immersed in different fluids. Interstitial tissue is immersed in the interstitial fluid that is derived from blood as a capillary filtrate. Seminiferous tubules are immersed in, the seminiferous or testicular fluid (TF). Sertoli cells contribute to the production of the TF that surrounds the seminiferous cells and contains hundreds of peptides, proteins and steroid hormones [24,25], which may be involved in crosstalk between germ cells and Sertoli cells. We developed an innovative strategy to enable us to study and decipher the germ cell secretome, with the aim of unraveling the molecular mechanisms underlying the crosstalk between Sertoli and germ cells. The TF proteomes of two species were analyzed by shotgun mass spectrometry and the results obtained were combined with those of transcriptome and theoretical secretome analyses on testicular seminiferous cells. This approach identified a set of dozens of genes encoding proteins present in the TF and potentially secreted by either Sertoli or germ cells. The integration of interactomics data then made it possible to detect potential interacting partners located on the surface of either germ cells or Sertoli cells. For the validation of our screening approach and candidate selection, we focused on two protein-protein interactions, which were confirmed *in situ* on rat testis sections, in proximity ligation assays (PLA).

Results

Experimental design and workflow

The primary objective of this study was to decipher the testicular germ cell secretome, which had previously been inaccessible, by analyzing the TF. The secondary objective was to highlight key proteins potentially involved in dialog between Sertoli and germ cells, focusing particularly on the proteins secreted by germ cells and involved in the regulation of Sertoli cell functions. We addressed these issues, by establishing a cross-species "integrative omics" workflow combining several types of large-scale data, as presented in Fig. 1. We first determined the core mammalian TF proteome, which we assumed would contain most of the diffusible factors involved in cell-cell crosstalk. We collected TF from male rats and rams. The TF was then fractionated and analyzed by shotgun proteomics methods, to identify as many of the proteins present in these complex biological fluids as possible. We used a gene expression dataset including the Sertoli and germ cell transcriptomes [26], to identify the candidate proteins unambiguously originating from particular seminiferous cell populations. We then focused on those genes preferentially expressed in one testicular cell type for which the corresponding gene product had been identified in the TF and that were known to encode actively secreted proteins; these genes were identified with the Secreted Protein Database [SPD; [27]]. In parallel, by combining the same seminiferous cell transcriptome dataset and the set of loci encoding plasma membrane or cell surface proteins, we assembled the individual testicular cell membranomes. We finally investigated whether physical protein-protein interactions between members of the Sertoli or germ cell secretome and members of the germ cell or Sertoli cell membranome had already been reported in other biological systems, using interactomic data from public repositories [see Materials and Methods; [28–31]].

Defining the mammalian TF proteome

We analyzed, compared and combined the sets of proteins identified in the TF of two mammalian species, *Rattus norvegicus* (rat) and *Ovis aries* (sheep), to build a reference map of the TF proteome in mammals. The rat is an established model organism for reproductive biology and toxicology, whereas the ram is a model of choice for studies on the hormonal control of reproduction [32–36]. The ram, with its large, accessible testes, was considered an ideal model for this project, as up to 20 to 25 ml of TF can be collected per testis in a given experiment from rams, whereas only 2 to 6 µl of TF per testis can be collected from rats.

We maximized the chances of picking up low-copy number proteins, by fractionating rat and ram TF before shotgun mass spectrometry analysis, by SDS-PAGE, after which the gel lanes were divided into 20 equal-sized pieces. The gel fragments were subjected to trypsin digestion and the resulting peptide digests were analyzed by nano-LC-MS/MS, generating 20 subproteomes. Overall, we identified 2,651 proteins in ram TF and 450 proteins in rat TF (UniProt identifiers (IDs)) [Fig. 2, panel A; PRIDE Proteomics Identifications database (http://www.ebi.ac.uk/pride); accession number: 31052-31111].

For direct comparisons of the two lists of gene products, the resulting UniProt IDs were sequentially matched with the corresponding gene entries (NCBI Entrez gene IDs), orthologous entries (HomoloGene IDs) and *Mus musculus* gene IDs. This strategy made it possible to decrease the redundancy of the identified proteins in a significant, unambiguous manner. We found that the 2,651 ram TF proteins and 450 rat TF proteins identified corresponded to 766 and 405 mouse genes, respectively (Entrez gene IDs). We next merged the two mouse gene lists and identified a total of 1,056 proteins (mouse Entrez gene IDs) present in TF from rat or ram. This dataset constitutes the first reference proteome for the mammalian TF (Fig. 2, panel A and table S1).

One sixth of the proteins identified in TF were preferentially produced by meiotic and post-meiotic germ cells

The TF is generated principally by Sertoli cells [37]. Sertoli cells clearly secrete active compounds into this fluid, but the release of soluble factors into the TF by germ cells has never been directly studied and documented. We investigated the contributions of the two cell types to TF content, by comparing the mammalian TF proteome characterized here with a previously published transcriptome [26] obtained with highly enriched populations of Sertoli cells, pachytene spermatocytes and round spermatids, from

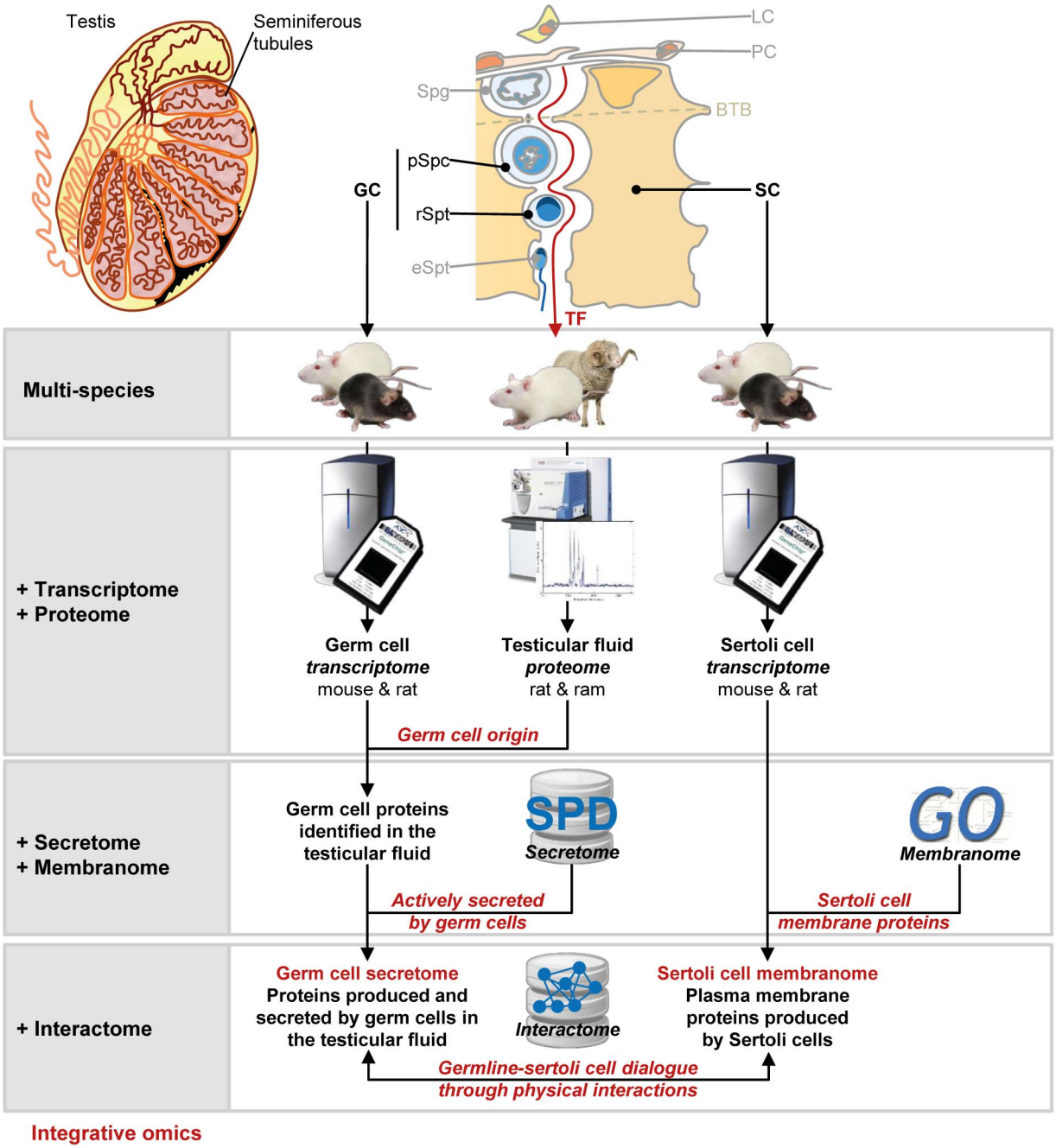

Figure 1. Experimental design and integrative omics workflow. A schematic diagram of the strategy used to access germ cell and Sertoli cell secretomes and to highlight potential protein-protein interactions. BTB: blood testis barrier; GC: germ cells; LC: Leydig cells; PC: peritubular cells; SC: Sertoli cells; Spg: spermatogonia; pSpc: pachytene spermatocytes; rSpt: round spermatids; eSPT: elongated spermatids.
doi:10.1371/journal.pone.0104418.g001

both mice and rats. We sought to integrate this expression dataset into our data, to distinguish between proteins originating preferentially from either the Sertoli cells or from the meiotic/post-meiotic germ cells. We first identified mouse and rat genes preferentially expressed in Sertoli cells rather than meiotic/post-meiotic germ cells, and in meiotic/post-meiotic germ cells rather than Sertoli cells (Fig. 2, panel B, see Materials and Methods). The rat gene IDs obtained for the rat expression dataset were converted into the corresponding mouse gene IDs. This statistical filtering process led to the definition of a germ-cell reference transcriptome composed of 3,923 mouse genes displaying significant differential expression between meiotic/post-meiotic germ cells and Sertoli cells. We also defined the Sertoli cell reference transcriptome, which consisted of 2,816 loci more strongly expressed in Sertoli cells than in germ cells (Fig. 2, panel B). We next focused on a subset of 177 loci preferentially expressed in germ cells (the germ-cell reference transcriptome) and encoding proteins present in the TF (the mammalian TF reference proteome) (Fig. 2, panel E). We then applied the same strategy to identify a subset of 150 genes preferentially expressed by Sertoli

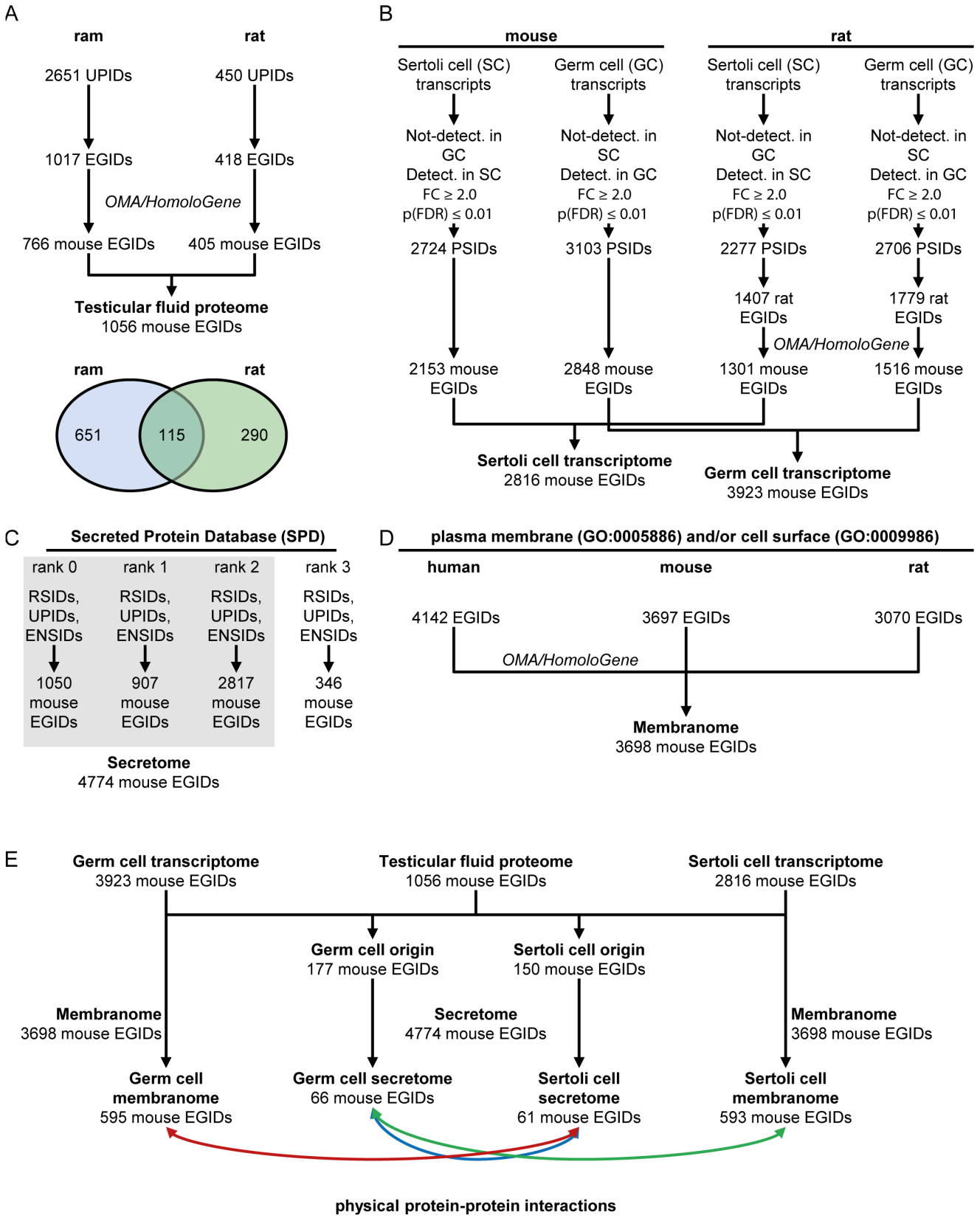

Figure 2. Details of datasets and the methods used to reconstruct dialog between Sertoli and germ cells. (A) Conversion of the rat and ram UniProt identifiers (UPIDs) into mouse Entrez Gene identifiers (EGIDs). (B) Definition of the germ cell and Sertoli cell transcriptomes (PSIDs: Probeset identifiers) (C) Selection of loci (mouse Entrez gene IDs) encoding secreted or potentially secreted proteins (RSIDs: RefSeq identifiers UPIDs: UniProt identifiers; ENSIDs: Ensembl identifiers) (D) Selection of genes encoding proteins associated with a "plasma membrane" and/or "cell surface"

location. (E) Selection of proteins secreted by one type of cell (germ or Sertoli cell) and interacting with membrane proteins of the other type of cell from BioGRID, HPRD, IntAct, MINT and NCBI databases.
doi:10.1371/journal.pone.0104418.g002

cells (i.e. present in both the Sertoli reference transcriptome and the TF reference proteome) (Fig. 2, panel E). About one sixth (177/1,056) of the 1,056 genes encoding proteins identified in the TF were preferentially expressed in meiotic/post-meiotic germ cells, and about one seventh (150/1,056) were preferentially expressed in Sertoli cells (table S1).

The set of proteins originating from germ cells and identified in TF displays significant enrichment in secreted factors

One of the key issues in this integrative genomics approach was determining the extent to which combining the TF reference proteome and the germ-cell (or Sertoli cell) reference transcriptome could help to identify the diffusible factors produced by germ cells (or Sertoli cells) and secreted into the TF. We therefore incorporated into the analysis a set of secreted factors from the SPD, in which the proteins are ranked according to a prediction confidence score of 0 to 3 [27]. We defined the reference secretome as mouse genes encoding proteins of ranks 0–2. This reference secretome consisted of 4,774 genes encoding known or predicted diffusible factors (Fig. 2, panel C; see Materials and Methods).

As expected, a significant proportion of the 747 loci encoding secreted proteins preferentially produced by germ cells was retrieved in the TF (66/177, $p<4.6\times10^{-9}$) (Fig. 2, panel E). Similarly, the list of genes expressed by Sertoli cells and encoding proteins identified in the TF was significantly enriched in genes encoding diffusible factors (61/150, $p<3.1\times10^{-6}$) (Fig. 2, panel E).

Prediction of the core molecular interactome, providing information about the cell-cell dialog occurring within the seminiferous tubules

We investigated potential physical protein-protein interactions between the secreted factors of germ cells and the membrane proteins of Sertoli cells, and vice versa. We first defined the germline and Sertoli cell membranomes, by selecting genes encoding cell surface proteins (Fig. 2, panel D) from the list of genes present in the reference transcriptome for the corresponding cell type (Fig. 2, panel B). We found that about 15% (595/3,923) and 21% (593/2,816) of the loci preferentially expressed in germ cells and Sertoli cells, respectively, were associated with gene products located on the plasma membrane (Fig. 2, panel E).

We investigated the extent to which factors secreted by one type of cell (meiotic/post-meiotic germ cells or Sertoli cells) into the TF interacted with cell surface proteins on the other type of cell, by combining cell-specific secretome data and cell-specific membranome data with information about protein-protein interactions. A graphical display created with AMEN [38] revealed a complex interlaced network of interactions between seminiferous cell types, mediated through the TF (Fig. 3). This large network consisted of 22 germ cell-secreted and 23 Sertoli cell-secreted factors interacting with 43 Sertoli cell and 69 germ cell membrane proteins. The physical associations highlighted by this analysis were supported by the findings of 140 published studies on various biological systems and model organisms. This network analysis identified well-known connections between germ cells and somatic cells, such as the intimate association of CLU (clusterin) with SPAM1 (sperm adhesion molecule 1) [39]. CLU is one of the major proteins secreted by Sertoli cells and it has already been associated with the surface of spermatozoa [40]. By contrast, SPAM1 is an important hyaluronidase secreted and acquired by spermatozoa, and playing a key role in fertilization [41,42].

Validation of the protein partners potentially involved in the dialog between Sertoli and germ cells

For the validation of our approach, we focused on proteins secreted by germ cells with potential partners expressed on the Sertoli cell membrane. We then investigated *in situ* two novel physical molecular interactions that had never before been reported in the testis and for which well characterized antibodies were commercially available: the interactions of APP (amyloid beta precursor protein) with NGFR (nerve growth factor receptor) and CDC42 (cell division cycle 42) with APOH (apolipoprotein H) [43,44]. We used the *in situ* PLA to visualize protein-protein interactions in fixed rat testis sections.

The PLA can be used to visualize the molecular proximity (<4 nm) between two proteins of interest directly on tissue slices [45]. For the APOH and CDC42 proteins, abundant PLA signals (red dots) were detected on testis sections with anti-APOH and anti-CDC42 antibodies (Fig. 4A). Significantly fewer PLA signals were detected if only one primary antibody (anti-APOH or anti-CDC42) was used (Figs. 4 B and C). These observations were confirmed by the quantification of PLA signals on testis sections (Fig. 4D), which presented a mean of 312 PLA signals/0.25 mm^2 for APOH/CDC42H interactions and 29 PLA signals/0.25 mm^2 for APOH alone or CDC42 alone. These results were statistically significant (Student's *t*-test $p<0.01$) and strongly suggest that APOH and CDC42 interact within the rat seminiferous tubules. Intriguingly, a nuclear signal independent of the PLA signal was observed in spermatids and spermatogonia on a few tubule sections (Fig. 4B). Similar results have already been reported for fixed tissues, on which the deleterious effects of aldehydes on DNA might favor the binding of fluorescent oligonucleotides during the PLA reaction [46]. This non-specific signal, which did not appear as dots, was not taken into account when we quantified PLA signals on testis sections.

For the APP and NGFR proteins, PLA showed numerous red dots on rat testis sections with anti-APP and anti-NGFR antibodies (Fig. 4E). A smaller number of PLA signals were observed if only one of these antibodies was used (Figs. 4F and G). The counting of PLA signals confirmed this observation, with the detection of a mean of 237 PLA signals/0.25 mm^2 in APP/NGFR conditions and of 80 PLA signals/0.25 mm^2 for APP alone or NGFR alone (Fig. 4H). These results were not statistically significant (Student's *t*-test $p = 0.16$), but they nevertheless strongly suggest that APP and NGFR interact within the rat seminiferous tubules.

Discussion

The primary aim of this study was to decipher the mammalian testicular germ cell secretome, which had previously not been technically possible. The maintenance of isolated germ cell populations in primary culture remains unsatisfactory. Indeed, following their isolation from rat or mouse testes, classical models in this field, a large proportion of germ cells are found to have already entered a preapoptotic process, with 40 to 60% positive for Annexin V staining (Pineau *et al.*, unpublished observation). Interestingly, germ cell apoptosis is a major event within the

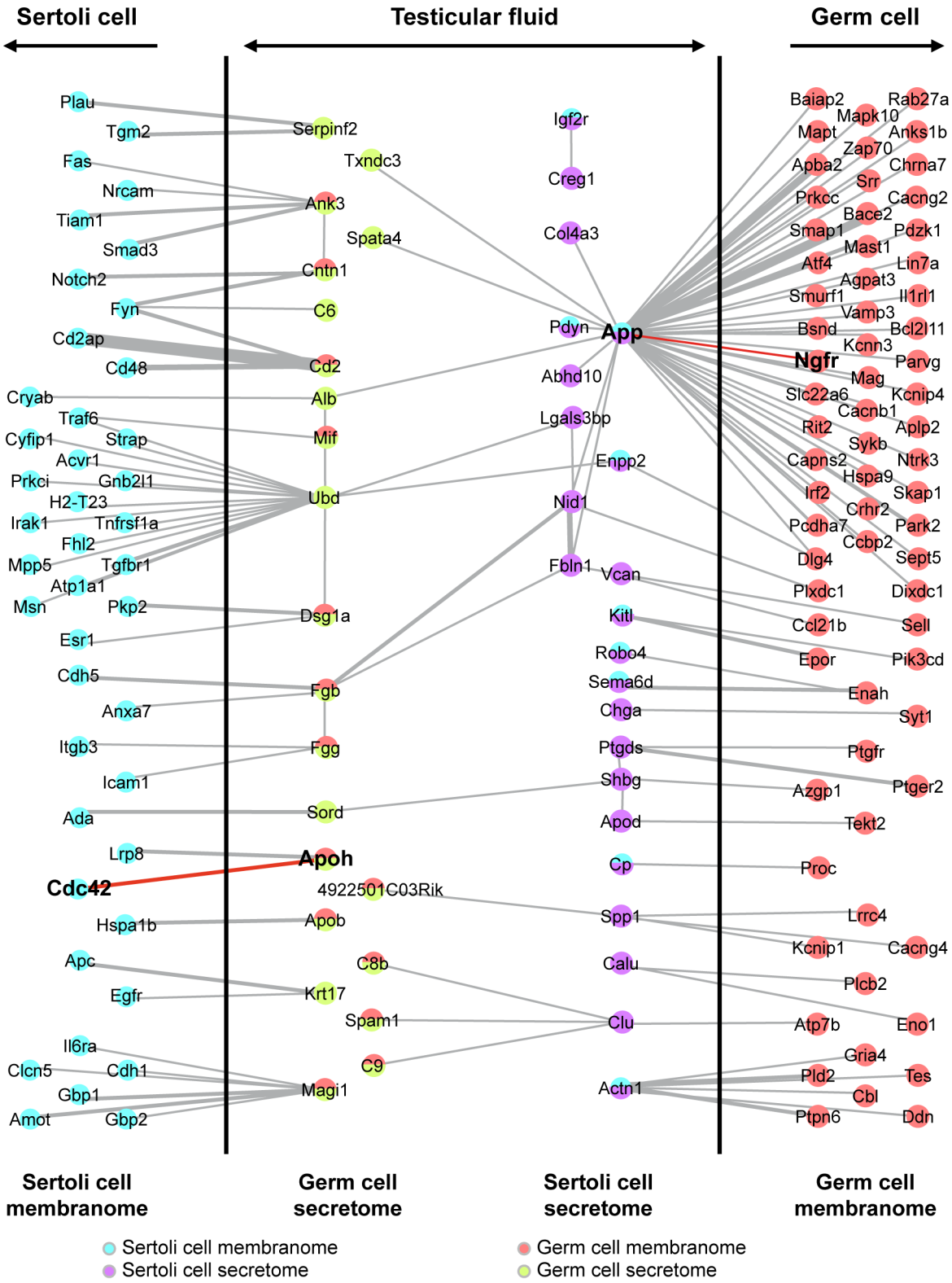

Figure 3. Integration of ''omics'' data to establish a network of molecular interactions between germ cells and Sertoli cells mediated by the TF. This integrated network focuses on proteins produced and secreted by germ cells (GCs) or Sertoli cells (SCs) and interacting with membrane proteins of the other type of cell. Nodes symbolizing GC-secreted and Sertoli cell-secreted factors are indicated in light green and purple, respectively, whereas GC-membrane and Sertoli cell-membrane proteins are represented by red and light blue nodes, respectively.
doi:10.1371/journal.pone.0104418.g003

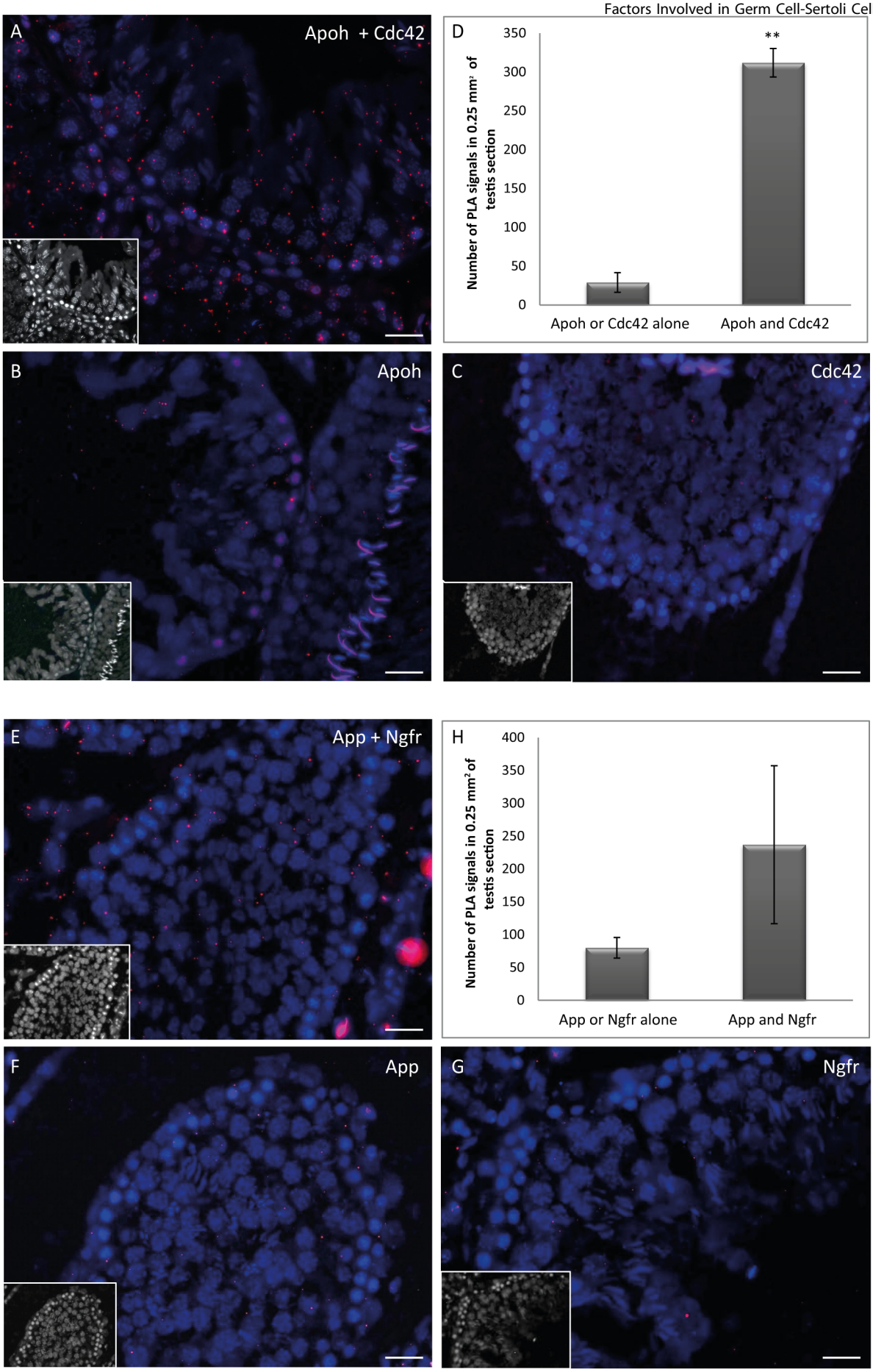
A
Apoh + Cdc42
B
Apoh
C
Cdc42
D
Number of PLA signals in 0.25 mm² of testis section
350
300
250
200
150
100
50
0
**
Apoh or Cdc42 alone
Apoh and Cdc42
E
App + Ngfr
F
App
G
Ngfr
H
Number of PLA signals in 0.25 mm² of testis section
400
350
300
250
200
150
100
50
0
App or Ngfr alone
App and Ngfr

Figure 4. *In situ* detection of APOH/CDC42 and APP/NGFR interactions in the rat testis by Duolink PLA. (A, E) Abundant PLA signals (red dots) were detected in the seminiferous tubules of rat testis when specific primary antibodies were used, reflecting the close proximity of APOH/CDC42 or APP/NGFR close proximity. (B, C, F, G) Negative controls, with only one primary antibody for the targeted protein-protein interaction. (D, H) Quantification of PLA signals in testis sections for APOH/CDC42 (** Student's *t*-test $p = 0.0016$) or for APP/NGFR (Student's *t*-test $p = 0.16$). Scale bars = 50 μm. A nonspecific background nuclear signal was observed for a few tubule sections (see B).
doi:10.1371/journal.pone.0104418.g004

seminiferous tubules and is undoubtedly linked to the spermatogenesis outcome. Thus, intracellular proteins in the conditioned culture medium may originate from either a physiological leakage or a degradation of isolated cells during the isolation procedures. In this context, germ cell secretomes cannot be deciphered from conditioned culture medium, because this medium contains cellular debris and a large number of intracellular proteins. Unfortunately, no immortalized germ cell line is currently available to overcome these limitations. However, a promising neonatal mouse testis culture method at the gas-liquid interface makes it possible to maintain a functional spermatogenesis *in vitro*. If needed, it could be adapted to other species (e.g., rat) with minor efforts. This innovative approach should offer great potential for studying molecular mechanisms in spermatogenesis [47–49]. Due to the problems described above, studies on the regulation of Sertoli cell function by germ cell-secreted proteins, a major field of research in the 1980s and 1990s, was considered to have reached a dead end [for a review see [3]].

Secreted factors constitute a major class of proteins defining the cellular secretome and acting as regulators of numerous biological and physiological processes, through paracrine or autocrine effects. Secretomics has, thus, rapidly become a key area of proteomics research, for the discovery of biomarkers and therapeutic targets in diseases [50,51]. Studies of diffusible factors are limited by: *i*) the difficulties isolating and growing many cell types in single primary cultures; *ii*) the need for coculture or cultures on specific substrates more closely reflecting the *in vivo* situation but calling for challenging experimental designs *iii*) the need to add fetal calf serum to culture medium, its removal by starvation being incomplete, masking the presence of low-abundance secreted proteins; *iv*) the use of immortalized cell lines, the secretion patterns of which may differ considerably from that of normal cells in primary culture [for a review see [52]]. Moreover, even under optimal culture conditions, it remains difficult to control cell damage and *in vitro* secretome studies have consistently shown that several intracellular proteins are released by cultured mammalian cells into the conditioned medium [53]. Many of these proteins may originate from cell death or leakage, but others may be secreted via non classical pathways, perhaps via vesicles and exosomes [54], and may have extracellular functions (e.g., α-enolase). The analysis of secretomes remains highly challenging, due to these technical issues. The development of alternative approaches is therefore required.

In this study, we developed an "integrative omics" strategy for studying the germ cell secretome through the analysis of TF, a complex biological fluid that surrounds germ and somatic cells within the seminiferous tubules and contains many secreted peptides, proteins and hormones [24,25]. Bortoluzzi *et al*. studied the skeletal muscle secretome, using a pioneering computational approach in which putatively secreted proteins were identified by sequential sieving, signal peptide prediction, the recognition of transmembrane regions and the analysis of protein annotation [55]. Similarly, a publicly available secreted protein database, the SPD, was specifically designed to define as exhaustive as possible a secretome for humans, mice and rats, and to rank the resulting known and predicted secreted factors into different categories, according to a homemade classification pipeline [27].

We were able to link 1,056 of the 2,651 ram TF proteins and 450 of the rat TF proteins to mouse Entrez gene IDs, reflecting the stringency of our approach. The smaller number of Entrez gene IDs than of proteins identified can be accounted for by: (*i*) the inherent redundancy of the multi-species protein sequence database (subset of the UniProt Knowledgebase for mammals), leading to the identification of several orthologous proteins/genes that were eventually linked to a single mouse Entrez gene ID; (*ii*), the absence of links to the Entrez gene or HomoloGene databases for some of the proteins identified.

As expected, our dataset included several proteins known to be secreted by Sertoli cells, such as inhibin-α, and the inhibin-βA and inhibin-β subunits, with a SPD rank of 0 corresponding to known secreted proteins. As target cells for follicle-stimulating hormone (FSH) within the testis, Sertoli cells finely tune the secretion of these subunits and production of the glycoprotein hormone — consisting of two partially homologous subunits (α and β) — which downregulates FSH secretion by the pituitary gland [56]. Inhibin is thus probably produced at a low abundance, explaining the detection of inhibin subunits in ram TF but not in rat TF, for which the amounts of material available for analysis were too small. Another protein preferentially secreted by Sertoli cells was the androgen-binding protein SHBG, historically considered to be a marker of Sertoli cell function [57]. ABP, a high-affinity carrier of androgens within the seminiferous tubules, is expressed at higher basal levels and was thus detected in the TF of both rats and rams, with a SPD rank of 1, corresponding to proteins with signal peptides predicted by both the PSORT and Sec-HMMER algorithms. Other markers of Sertoli cell function detected with high secretion scores, were clusterin, α2-macroglobulin and AMH [for a review, see [3]]. Sertoli cells are easy to maintain in primary culture, and their secretome can therefore be studied by the conventional *in vitro* approach. Our strategy identified a large number of putative secreted proteins from both the germ cell and Sertoli cell lineages, but we exploited only part of this valuable dataset for this study, focusing on the germ cell secretome. We identified 66 germ cell-secreted proteins, constituting the first theoretical secretome established for testicular seminiferous tubule cells and, in particular, for germ cells. We are now working to validate these candidates and their potential partners and to understand their role in spermatogenesis.

Two of the proposed protein-protein interactions highlighted in this study were validated in PLA (Duolink). In our view, the colocalization of two proteins with specific antibodies, even by confocal microscopy, does not provide conclusive proof that the two proteins interact physically. Several approaches for assessing protein-protein interactions are available, including the well known yeast two-hybrid assay, co-immunoprecipitation and tandem affinity purification followed by mass spectrometry characterization. These techniques can yield valuable information, but they do not explain how proteins interact within cells. Förster resonance energy transfer (FRET)-based methods [58] and protein-fragment complementation assays (PCA) provide interesting alternative approaches to studying protein-protein interactions in living cells [59]. However, both these methods are based on protein tagging and the need for the time-consuming production of molecular constructs (for a review see [60]). For this reason, we

used the protein ligation assay, which has a number of advantages over these methods because it can be used for *in situ* interaction analyses for any protein for which specific antibodies are available. In this context, recognition by two or more binding reagents ensures a high degree of specificity [60].

The interaction between APOH and CDC42 has been demonstrated before, with yeast two-hybrid technology [44]. These two proteins play crucial roles in spermatogenesis, but their interaction in the testis has never before been reported. CDC42 is a plasma membrane-associated small GTPase involved in the regulation of Sertoli cell polarity, cell adhesion at both the blood-testis barrier and the apical ectoplasmic specialization structure, and regulation of the dynamics of the blood-testis barrier [61,62]. Beta-2-glycoprotein 1, officially known as APOH, is a protein that binds to various kinds of negatively charged substances, such as phospholipids, thus playing a critical role in the clearance of liposomes from the blood [63,64]. It has been detected in the testis, at a time point corresponding to the appearance of mature germ cells and the completion of spermatogenesis, suggesting a role in apoptotic body clearance during spermatogenesis [65,66]. We found that APOH was detectable in TF, secreted by meiotic/post-meiotic germ cells and potentially interacted with CDC42 at the Sertoli cell membrane. Cell junctions in the seminiferous epithelium are dynamic structures involved in signal transduction events [67], so the APOH/CDC42 interaction may be involved in communication between germ cells and Sertoli cells at late stages of spermatogenesis, thereby facilitating the endocytosis of residual bodies by Sertoli cells.

The NGFR, also known as p75NTR, is an alternative receptor to APP in neurons [43,68]. The testis has been shown to contain both these proteins, but their interaction has never before been reported in this organ. APP is a transmembrane protein, the cleavage of which generates peptides, some of which are associated with Alzheimer's disease. APP is produced by cells with a high membrane fusion activity (*i.e.*, membrane turnover activity), including Sertoli cells [69], suggesting a role in the maintenance of cellular integrity. In other studies, APP has been detected in the acrosome and the growing tail of spermatids in rat seminiferous tubules [70] and in the head and tail of human spermatozoa [71], suggesting a role in sperm function. Several studies have reported the expression of NGFR in various testicular cell types, including pachytene spermatocytes and round spermatids [72,73]. We show here that APP, which is potentially secreted into the TF by Sertoli cells, interacts with NGFR at the membrane of meiotic and post-meiotic germ cells, consistent with a potential role in the regulation of male germ cell development and spermiogenesis.

Our results provide new insight into the extracellular factors potentially involved in correctly establishing essential communication between germ cells and Sertoli cells. Using a conventional *in vitro* culture approach, Flenkenthaler *et al*. [74] recently established the secretome of human testicular peritubular cells and suggested that these cells played a crucial role in maintaining an appropriate microenvironment in the spermatogonial stem cell niche, through the secretion of proteins involved in cell adhesion and migration. We show here that combining three types of omics data results in the accurate identification of potential cell-specific diffusible factors in a complex biological fluid composed of secretions from several cell types. One has to keep in mind that spermatogenesis is a highly synchronized process in which fine regulation takes place along the cycle of the seminiferous epithelium. As a consequence, cell secretomes should vary at each stage of the spermatogenic cycle, leading to a dynamic and specific protein composition of the TF microenvironment along the tubules. In such context, only a global secretome analysis of seminiferous tubules cells could be performed here. Indeed, the approach used was not meant to characterize proteins involved in Sertoli-germ cells communication at each specific stage of the spermatogenic cycle. Moreover the protein dataset presented here is that of the TF collected at the rete testis. It could be slightly different from that of a TF collected elsewhere, as the rete testis is atypical of seminiferous tubules, as specific functions and is likely to contain specific proteins. Our results confirm nevertheless that it is now possible to study cell secretomes that were previously inaccessible, by a computational approach overcoming the limitations of *in vitro* culture-based methods. We are currently investigating these interactions further, by conventional biological and biochemical approaches, and are also validating several other potential partners, to increase our understanding of the crosstalk between germ cells and Sertoli cells during spermatogenesis. This integrative strategy could be used more widely, to study other cell secretomes and to elucidate meaningful molecular mechanisms underlying cell-cell communication.

Materials and Methods

Animals and collection of testicular rete testis fluids

Animal experimentations were approved by the local Veterinary Departments of the Departmental Direction of the Protection of the Populations (Ille et Vilaine DDCSPP, Rennes, France and Indre et Loire DDPP, Tours, France). Sprague-Dawley rats for the various experiments were purchased from Elevage Janvier (Le Genest Saint Isle, France). Ile-de-France rams were provided by the INRA-UMR85 experimental unit (Nouzilly, France). Rat TF was collected by microsurgery 24 h after rete testis ligature, as previously described [75]. Ram TF was collected from several animals by *in vivo* rete testis cannulation, as previously described [36]. TF was collected from each ram over a period of 12 hours. Spermatozoa were separated by centrifugation at $15000\times g$ for 20 minutes at 4°C. The supernatant was stored at −20°C until use. Proteomic analysis was carried out with a pool of equal amounts of TF from five rams.

Protein separation and digestion

TF was thawed and centrifuged for 15 minutes at $3000\times g$ and protein concentration was determined by the Bradford method (Bio-Rad, Marnes-la-Coquette, France). Samples were fractionated by SDS-PAGE in a 12% acrylamide precast gel (Invitrogen, Saint Aubin, France). The gel was then stained with Coomassie Blue G-250, with the EZBlue gel-staining reagent (Sigma-Aldrich, Saint-Quentin Fallavier, France). The entire gel lane was excised and cut into 20 bands, which were washed with various ACN/100 mM NH_4HCO_3 solutions. In-gel digestion was performed overnight at 37°C with modified trypsin (Promega, Charbonnières Les Bains, France), according to a previously described protocol [76]. Proteolytic peptides were then extracted from the gel by sequential incubation, using routine procedures, and extracts were concentrated to a final volume of 20 µl by evaporation.

Mass spectrometry analysis

Peptide mixtures were analyzed with a nanoflow high-performance liquid chromatography (HPLC) system (LC Packings Ultimate 3000, Thermo Fisher Scientific, Courtaboeuf, France) connected to a hybrid LTQ-OrbiTrap XL (Thermo Fisher Scientific) equipped with a nanoelectrospray ion source (New Objective), as previously described [77]. The mass spectrometer was operated in the data-dependent mode by automatic switching between full-survey scan MS and consecutive MS/MS acquisition. Survey full-scan MS spectra (mass range: 400–2000) were acquired

in the OrbiTrap section of the instrument, with a resolution of $r = 60{,}000$ at m/z 400; ion injection times were calculated for each spectrum, to allow for the accumulation of 10^6 ions in the OrbiTrap. The seven peptide ions giving the most intense signal in each survey scan, with an intensity above 2000 counts (to avoid triggering fragmentation too early in the peptide elution profile) and a charge state ≥ 2 were sequentially isolated at a target value of 10,000 and fragmented in the linear ion trap by collision-induced dissociation. The normalized collision energy was set to 35%, with an activation time of 30 milliseconds. Peaks selected for fragmentation were automatically placed on a dynamic exclusion list for 120 s with a mass tolerance of ± 10 ppm, to prevent the selection of the same ion for fragmentation more than once. The following parameters were used: the repeat count was set to 1, the exclusion list size limit was 500, singly charged precursors were rejected, and a maximum injection time of 500 ms and 300 ms for full MS and MS/MS scan events, respectively, was set. For an optimal duty cycle, the fragment ion spectra were recorded in the LTQ mass spectrometer in parallel with OrbiTrap full-scan detection. For OrbiTrap measurements, an external calibration was used before each injection series, giving an overall error for mass accuracy of less than 5 ppm for the detected peptides. MS data were saved in RAW file format (Thermo Fisher Scientific), with XCalibur 2.0.7 version 2.4.

Protein identification

Data were analyzed with Proteome Discoverer 1.2 software, with the Mascot (Matrixscience) and SEQUEST database search engines for peptide and protein identification. MS/MS spectra were used as queries to search the UniProt Database (Release 2010_07) restricted to Mammalia (121,346,285 residues; 330267 sequences). Mass tolerance was set to 10 ppm and 0.5 Daltons for MS and MS/MS, respectively. Enzyme selectivity was set to full trypsin, with one missed cleavage allowed. The allowed protein modifications were fixed carbamidomethylation of cysteines and variable oxidation of methionine, and variable phosphorylation of serine, threonine and tyrosine. Identified peptides were filtered on the basis of Xcorr values and Mascot score, to obtain a false discovery rate of 1% and a false positive rate of 5%. Proteome Discoverer was used to create a unique list of identified proteins per band. Redundancy was avoided by grouping proteins with shared peptides and displaying only the protein with the best score or the highest sequence coverage for a given group.

Data repository

Mascot protein identification data (.dat files) were converted into PRIDE xml files with the Pride Converter 2 Tool Suite (v.2.0.19,[78]) and submitted to the PRIDE Proteomics Identifications database (http://www.ebi.ac.uk/pride; [79]). Data are accessible under the project names "Proteomic characterization of ram testicular fluid" and "Proteomic characterization of rat testicular fluid" (accession number: 31052-31111).

Proteomic data analysis

For definition of the mammalian TF proteome (Fig. 2, panel A), all UniProt accession numbers corresponding to the proteins identified were linked to their corresponding gene IDs (NCBI Entrez gene IDs), which were subsequently mapped to the corresponding mouse gene IDs by HomoloGene [80] and to OMA [81] IDs with Annotation, Mapping, Expression and Network (AMEN) analysis software [38]. *Mus musculus* was selected as the reference species because more extensive annotation data are available for this species than for rat or sheep.

Transcriptomic data analysis

For definition of the transcriptomes of both Sertoli and germ cells (Fig. 2, panel B), we made use of a transcriptomic dataset including two populations of germ cells enriched in different types of cell (pachytene spermatocytes and round spermatids) and one population of Sertoli cells, based on a previously published Affymetrix GeneChip microarray analysis (Mouse 430 2.0 and rat 230 2.0 GeneChips) on mouse and rat [26] (ArrayExpress ID: E-TABM-130). Data were analyzed with AMEN. For identification of the testicular transcripts preferentially expressed in germ cells rather than Sertoli cells, we selected probe sets if at least one intensity value across germline samples (spermatocytes or spermatids) exceeded the background expression cutoff (BEC$\sim$6.1, corresponding to the overall median log2-transformed intensity). We avoided the inclusion of probe sets with signal values close to the BEC, by selecting only those with intensities at least twice the BEC. A LIMMA statistical test (F-value adjusted by the false discovery rate method: $p \leq 0.01$) was used to select probe sets displaying statistically significant changes. A similar strategy was used to define the Sertoli cell transcriptome, with the selection of probe sets yielding a signal above the BEC in Sertoli cell samples, with a fold-change ≥ 2.0 with respect to the germ cell signal and a p-value≤ 0.01. The selected probe set IDs were then linked to the corresponding gene IDs (NCBI Entrez gene IDs) with AMEN. Rat gene IDs were sequentially converted into OMA and HomoloGene IDs and then, finally, into mouse gene IDs. Any mouse gene IDs associated with several probe set IDs with opposite expression patterns (e.g. in both the germ cell and Sertoli cell transcriptomes) were discarded from the analysis.

Secretome and membranome data analysis

For the definition of a set of proteins actively secreted outside the cell membrane, otherwise known as a secretome (Fig. 2, panel C), we made use of a comprehensive collection of mouse secreted proteins via a web-accessible resource called SPD [27]. This database consists of a core dataset of $\sim$18,000 secreted proteins retrieved from Swiss-Prot/TrEMBL, Ensembl, RefSeq, and ranked according to the confidence associated with the prediction of their secretion, from rank 0 to 3. Briefly, proteins of rank 0 correspond to known secreted proteins in Swiss-Prot; rank 1 corresponds to proteins with a signal peptides predicted by both PSORT and Sec-HMMER; rank 2 corresponds to proteins with signal peptides predicted by either PSORT or Sec-HMMER; and rank 3 corresponds to proteins with a signal peptide of more than 70 amino acids predicted by Sec-HMMER only. We did not consider rank 3 proteins in our analysis. Mouse protein IDs of ranks 0-2 were converted into their corresponding mouse Entrez gene IDs.

Human, mouse and rat genes encoding membrane proteins, corresponding to the membranome, were selected on the basis of their association with the "cell surface" (GO:0009986) and "plasma membrane" (GO:0005886) Gene Ontology terms in the 'gene2go' file downloaded from the NCBI website (Fig. 2, panel D). The selected human and rat gene IDs were converted to the corresponding mouse gene IDs via HomoloGene and OMA IDs.

Integrative omics data analysis

The germ cell (or Sertoli cell) secretome (Fig. 2, panel E) — the genes (mouse Entrez gene IDs) expressed in germ cells (or Sertoli cells) and encoding proteins actively secreted into TF — was determined by the intersection of three types of omics data: (i) the germ cell (or Sertoli cell) transcriptome; (ii) the secretome; and (iii) the TF proteome.

The Sertoli cell (or germ cell) membranome (Fig. 2, panel E) — the genes (mouse Entrez gene IDs) expressed in Sertoli cells (or germ cells) and encoding membrane proteins — was determined by the intersection of two types of omics data: (i) the Sertoli cell (or germ cell) transcriptome; and, (ii) the membranome.

Finally, we investigated dialog between germ cells and Sertoli cells by focusing on interactomic data describing physical interactions between the proteins of the secretome of one type of cell (germ cell or Sertoli cell) and those of the membranome or secretome of the other type of cell.

Interactomic data analysis

Physical protein-protein interaction data were downloaded from the BioGRID, HPRD, IntAct, MINT and NCBI databases [28–31]. The physical associations explored in this study correspond to a consolidation of all mammalian datasets. Briefly, all mammalian protein IDs were converted into mouse gene IDs via the OMA and HomoloGene databases. A representation of the network was drawn with AMEN software and edited by hand.

In situ proximity ligation assay (PLA)

Bouin reagent-fixed and paraffin-embedded rat testes were prepared as previously described [82]. Antigens were retrieved by heating for 10 minutes in a microwave oven, in citrate buffer (10 mM, pH 6.0, 0.05% Tween 20) for APOH/CDC42 couple, or in Tris-EDTA buffer (10 mM Tris, 1 mM EDTA, pH 9.0, 0.05% Tween 20) for APP/NGFR. Antibodies directed against ApoH (LS-B2591 goat polyclonal antibody, LifeSpan Biosciences, Inc., Seattle, USA), CDC42 (ab64533 rabbit polyclonal antibody, Abcam, Cambridge, UK), APP (rabbit polyclonal antibody, Abnova, Taipei City, Taiwan) and NGFR (mouse monoclonal antibody, Osenses Pty Ltd, Keswick, Australia) were used at the following concentrations: 2.5 µg/ml, 5 µg/ml, a dilution of 1/200 and 5 µg/ml respectively. We used a Duolink II *in situ* PLA kit with PLA probes anti-rabbit PLUS and anti-goat MINUS or PLA probes anti-rabbit PLUS and anti-mouse MINUS (OLINK Bioscience, Uppsala, Sweden) for the detection of APOH/CDC42 or APP/NGFR interactions *in situ*, respectively, according to the manufacturer's instructions. Complex formation was detected with Duolink II Detection Reagents Far Red (OLINK Bioscience, Uppsala, Sweden) and a DMRXA2 microscope (Leica Microsystèmes SAS, Nanterre, France).

Supporting Information

Table S1 Lists the core reference proteome of the mammalian testicular fluid (TF).
(XLSX)

Acknowledgments

We thank Bertrand Evrard, Christine Kervarrec and Dr Florence Aubry for preparing histology materials and assistance in the optimization of immunochemistry experiments. We thank Dr Nathalie Melaine for valuable advice and assistance with Duolink image acquisition and processing. Duolink images were acquired with a microscope from the Microscopy Rennes Imaging Center (MRic-ALMF; UMS 6480 Biosit, Rennes, France).

Author Contributions

Conceived and designed the experiments: CP EC FC. Performed the experiments: APT JLD NH RL FC EC. Analyzed the data: FC EC NH. Contributed reagents/materials/analysis tools: APT JLD NH RL FC EC CP. Contributed to the writing of the manuscript: CP FC EC.

References

1. Clermont Y (1972) Kinetics of spermatogenesis in mammals: seminiferous epithelium cycle and spermatogonial renewal. Physiol Rev 52: 198–236.
2. Jegou B (1993) The Sertoli-germ cell communication network in mammals. Int Rev Cytol 147: 25–96.
3. Jégou B, Pineau C, Dupaix A (1999) Paracrine control of testis function. In: Wang C, editor. Male Reproductive Function. Berlin: Kluwer Academic. pp. 41–64.
4. Jégou B, Sharpe RM (1993) Paracrine mechanisms in testicular control. In: DM dK, editor. Molecular Biology of the Male Reproduction System. New York: Academic Press. pp. 271–310.
5. Sharpe RM (1994) Regulation of spermatogenesis. In: Knobil EaN, J D., editor. The Physiology of Reproduction 2nd edition. New York: Lippincott Williams & Wilkins.
6. Eddy EM (2002) Male germ cell gene expression. Recent Prog Horm Res 57: 103–128.
7. Griswold MD (1995) Interactions between germ cells and Sertoli cells in the testis. Biol Reprod 52: 211–216.
8. de Rooij DG (2001) Proliferation and differentiation of spermatogonial stem cells. Reproduction 121: 347–354.
9. Sertoli E (1865) Dell'esistenza di particolari cellule ramificate nei canalicoli seminiferi del testicolo umano. Morgagni 7: 31–39.
10. Pineau C, Syed V, Bardin CW, Jegou B, Cheng CY (1993) Germ cell-conditioned medium contains multiple factors that modulate the secretion of testins, clusterin, and transferrin by Sertoli cells. J Androl 14: 87–98.
11. Le Magueresse B, Pineau C, Guillou F, Jegou B (1988) Influence of germ cells upon transferrin secretion by rat Sertoli cells in vitro. J Endocrinol 118: R13–16.
12. Pineau C, Velez de la Calle JF, Pinon-Lataillade G, Jegou B (1989) Assessment of testicular function after acute and chronic irradiation: further evidence for an influence of late spermatids on Sertoli cell function in the adult rat. Endocrinology 124: 2720–2728.
13. Onoda M, Djakiew D (1993) A 29,000 M(r) protein derived from round spermatids regulates Sertoli cell secretion. Mol Cell Endocrinol 93: 53–61.
14. Matzuk MM, Lamb DJ (2002) Genetic dissection of mammalian fertility pathways. Nat Cell Biol 4 Suppl: s41–49.
15. de Rooij DG, de Boer P (2003) Specific arrests of spermatogenesis in genetically modified and mutant mice. Cytogenet Genome Res 103: 267–276.
16. Wrobel G, Primig M (2005) Mammalian male germ cells are fertile ground for expression profiling of sexual reproduction. Reproduction 129: 1–7.
17. Rolland AD, Jegou B, Pineau C (2008) Testicular development and spermatogenesis: harvesting the postgenomics bounty. Adv Exp Med Biol 636: 16–41.
18. Chalmel F, Lardenois A, Primig M (2007) Toward understanding the core meiotic transcriptome in mammals and its implications for somatic cancer. Ann N Y Acad Sci 1120: 1–15.
19. Calvel P, Rolland AD, Jegou B, Pineau C (2010) Testicular postgenomics: targeting the regulation of spermatogenesis. Philos Trans R Soc Lond B Biol Sci 365: 1481–1500.
20. Chocu S, Calvel P, Rolland AD, Pineau C (2012) Spermatogenesis in mammals: proteomic insights. Syst Biol Reprod Med 58: 179–190.
21. Rolland AD, Lavigne R, Dauly C, Calvel P, Kervarrec C, et al. (2013) Identification of genital tract markers in the human seminal plasma using an integrative genomics approach. Hum Reprod 28: 199–209.
22. Guyonnet B, Dacheux F, Dacheux JL, Gatti JL (2011) The epididymal transcriptome and proteome provide some insights into new epididymal regulations. J Androl 32: 651–664.
23. Soumillon M, Necsulea A, Weier M, Brawand D, Zhang X, et al. (2013) Cellular source and mechanisms of high transcriptome complexity in the mammalian testis. Cell Rep 3: 2179–2190.
24. Setchell BP (1967) Fluid secretion by the testis. J Reprod Fertil 14: 347–348.
25. Setchell BP, Waites GM (1971) The exocrine secretion of the testis and spermatogenesis. J Reprod Fertil Suppl 13: 15–27.
26. Chalmel F, Rolland AD, Niederhauser-Wiederkehr C, Chung SS, Demougin P, et al. (2007) The conserved transcriptome in human and rodent male gametogenesis. Proc Natl Acad Sci U S A 104: 8346–8351.
27. Chen Y, Zhang Y, Yin Y, Gao G, Li S, et al. (2005) SPD—a web-based secreted protein database. Nucleic Acids Res 33: D169–173.
28. Stark C, Breitkreutz BJ, Chatr-Aryamontri A, Boucher L, Oughtred R, et al. (2011) The BioGRID Interaction Database: 2011 update. Nucleic Acids Res 39: D698–704.
29. Kerrien S, Aranda B, Breuza L, Bridge A, Broackes-Carter F, et al. (2012) The IntAct molecular interaction database in 2012. Nucleic Acids Res 40: D841–846.
30. Licata L, Briganti L, Peluso D, Perfetto L, Iannuccelli M, et al. (2012) MINT, the molecular interaction database: 2012 update. Nucleic Acids Res 40: D857–861.

31. Keshava Prasad TS, Goel R, Kandasamy K, Keerthikumar S, Kumar S, et al. (2009) Human Protein Reference Database—2009 update. Nucleic Acids Res 37: D767–772.
32. Jegou B, Dacheux JL, Terqui M, Garnier DH, Courot M (1978) Studies of the androgen binding protein in the rete testis fluid of the ram and its relation to sexual season. Mol Cell Endocrinol 9: 335–346.
33. Cahoreau C, Blanc MR, Dacheux JL, Pisselet C, Courot M (1979) Inhibin activity in ram rete testis fluid: depression of plasma FSH and LH in the castrated and cryptorchid ram. J Reprod Fertil Suppl: 97–116.
34. Courot M, Hochereau-de-Reviers MT, Monet-Kuntz C, Locatelli A, Pisselet C, et al. (1979) Endocrinology of spermatogenesis in the hypophysectomized ram. J Reprod Fertil Suppl: 165–173.
35. Jegou B, Dacheux JL, Garnier DH, Terqui M, Colas G, et al. (1979) Biochemical and physiological studies of androgen-binding protein in the reproductive tract of the ram. J Reprod Fertil 57: 311–318.
36. Dacheux JL, Pisselet C, Blanc MR, Hochereau-de-Reviers MT, Courot M (1981) Seasonal variations in rete testis fluid secretion and sperm production in different breeds of ram. J Reprod Fertil 61: 363–371.
37. Setchell BP (1969) Do Sertoli cells secrete fluid into the seminiferous tubules? J Reprod Fertil 19: 391–392.
38. Chalmel F, Primig M (2008) The Annotation, Mapping, Expression and Network (AMEN) suite of tools for molecular systems biology. BMC Bioinformatics 9: 86.
39. Griffiths GS, Galileo DS, Aravindan RG, Martin-DeLeon PA (2009) Clusterin facilitates exchange of glycosyl phosphatidylinositol-linked SPAM1 between reproductive luminal fluids and mouse and human sperm membranes. Biol Reprod 81: 562–570.
40. Law GL, Griswold MD (1994) Activity and form of sulfated glycoprotein 2 (clusterin) from cultured Sertoli cells, testis, and epididymis of the rat. Biol Reprod 50: 669–679.
41. Martin-DeLeon PA (2006) Epididymal SPAM1 and its impact on sperm function. Mol Cell Endocrinol 250: 114–121.
42. Martin-Deleon PA (2011) Germ-cell hyaluronidases: their roles in sperm function. Int J Androl 34: e306–318.
43. Nikolaev A, McLaughlin T, O'Leary DD, Tessier-Lavigne M (2009) APP binds DR6 to trigger axon pruning and neuron death via distinct caspases. Nature 457: 981–989.
44. Wang J, Yuan Y, Zhou Y, Guo L, Zhang L, et al. (2008) Protein interaction data set highlighted with human Ras-MAPK/PI3K signaling pathways. J Proteome Res 7: 3879–3889.
45. Soderberg O, Leuchowius KJ, Gullberg M, Jarvius M, Weibrecht I, et al. (2008) Characterizing proteins and their interactions in cells and tissues using the in situ proximity ligation assay. Methods 45: 227–232.
46. Trifilieff P, Rives ML, Urizar E, Piskorowski RA, Vishwasrao HD, et al. (2011) Detection of antigen interactions ex vivo by proximity ligation assay: endogenous dopamine D2-adenosine A2A receptor complexes in the striatum. Biotechniques 51: 111–118.
47. Sato T, Katagiri K, Gohbara A, Inoue K, Ogonuki N, et al. (2011) In vitro production of functional sperm in cultured neonatal mouse testes. Nature 471: 504–507.
48. Sato T, Katagiri K, Yokonishi T, Kubota Y, Inoue K, et al. (2011) In vitro production of fertile sperm from murine spermatogonial stem cell lines. Nat Commun 2: 472.
49. Sato T, Katagiri K, Kubota Y, Ogawa T (2013) In vitro sperm production from mouse spermatogonial stem cell lines using an organ culture method. Nat Protoc 8: 2098–2104.
50. Hathout Y (2007) Approaches to the study of the cell secretome. Expert Rev Proteomics 4: 239–248.
51. Brown KJ, Seol H, Pillai DK, Sankoorikal BJ, Formolo CA, et al. (2013) The human secretome atlas initiative: implications in health and disease conditions. Biochim Biophys Acta 1834: 2454–2461.
52. Brown KJ, Formolo CA, Seol H, Marathi RL, Duguez S, et al. (2012) Advances in the proteomic investigation of the cell secretome. Expert Rev Proteomics 9: 337–345.
53. Zwickl H, Traxler E, Staettner S, Parzefall W, Grasl-Kraupp B, et al. (2005) A novel technique to specifically analyze the secretome of cells and tissues. Electrophoresis 26: 2779–2785.
54. Nickel W (2010) Pathways of unconventional protein secretion. Curr Opin Biotechnol 21: 621–626.
55. Bortoluzzi S, Scannapieco P, Cestaro A, Danieli GA, Schiaffino S (2006) Computational reconstruction of the human skeletal muscle secretome. Proteins 62: 776–792.
56. De Jong FH (1988) Inhibin. Physiol Rev 68: 555–607.
57. Cheng SL, Wright W, Musto N, Gunsalus G, Bardin CW (1982) Testicular proteins which can be used to study seminiferous tubular function: a study of ABP and other testis-specific markers. Prog Clin Biol Res 87: 193–216.
58. Sekar RB, Periasamy A (2003) Fluorescence resonance energy transfer (FRET) microscopy imaging of live cell protein localizations. J Cell Biol 160: 629–633.
59. Michnick SW, Ear PH, Manderson EN, Remy I, Stefan E (2007) Universal strategies in research and drug discovery based on protein-fragment complementation assays. Nat Rev Drug Discov 6: 569–582.
60. Gullberg M, Fredriksson S, Taussig M, Jarvius J, Gustafsdottir S, et al. (2003) A sense of closeness: protein detection by proximity ligation. Curr Opin Biotechnol 14: 82–86.
61. Wong EW, Cheng CY (2009) Polarity proteins and cell-cell interactions in the testis. Int Rev Cell Mol Biol 278: 309–353.
62. Wong EW, Mruk DD, Lee WM, Cheng CY (2010) Regulation of blood-testis barrier dynamics by TGF-beta3 is a Cdc42-dependent protein trafficking event. Proc Natl Acad Sci U S A 107: 11399–11404.
63. Chonn A, Semple SC, Cullis PR (1995) Beta 2 glycoprotein I is a major protein associated with very rapidly cleared liposomes in vivo, suggesting a significant role in the immune clearance of "non-self" particles. J Biol Chem 270: 25845–25849.
64. Ishida T, Harashima H, Kiwada H (2002) Liposome clearance. Biosci Rep 22: 197–224.
65. Giuffrida V, Pezzino FM, Romano F, Litrico L, Garofalo MR, et al. (2006) Gene expression in mouse spermatogenesis during ontogenesis. Int J Mol Med 17: 523–528.
66. Shima JE, McLean DJ, McCarrey JR, Griswold MD (2004) The murine testicular transcriptome: characterizing gene expression in the testis during the progression of spermatogenesis. Biol Reprod 71: 319–330.
67. Mruk DD, Cheng CY (2004) Sertoli-Sertoli and Sertoli-germ cell interactions and their significance in germ cell movement in the seminiferous epithelium during spermatogenesis. Endocr Rev 25: 747–806.
68. Hasebe N, Fujita Y, Ueno M, Yoshimura K, Fujino Y, et al. (2013) Soluble beta-amyloid Precursor Protein Alpha Binds to p75 Neurotrophin Receptor to Promote Neurite Outgrowth. PLoS One 8: e82321.
69. Beer J, Masters CL, Beyreuther K (1995) Cells from peripheral tissues that exhibit high APP expression are characterized by their high membrane fusion activity. Neurodegeneration 4: 51–59.
70. Shoji M, Kawarabayashi T, Harigaya Y, Yamaguchi H, Hirai S, et al. (1990) Alzheimer amyloid beta-protein precursor in sperm development. Am J Pathol 137: 1027–1032.
71. Fardilha M, Vieira SI, Barros A, Sousa M, Da Cruz e Silva OA, et al. (2007) Differential distribution of Alzheimer's amyloid precursor protein family variants in human sperm. Ann N Y Acad Sci 1096: 196–206.
72. Li C, Zhou X (2013) The potential roles of neurotrophins in male reproduction. Reproduction 145: R89–95.
73. Perrard MH, Vigier M, Damestoy A, Chapat C, Silandre D, et al. (2007) beta-Nerve growth factor participates in an auto/paracrine pathway of regulation of the meiotic differentiation of rat spermatocytes. J Cell Physiol 210: 51–62.
74. Flenkenthaler F, Windschuttl S, Frohlich T, Schwarzer JU, Mayerhofer A, et al. (2014) Secretome analysis of testicular peritubular cells: a window into the human testicular microenvironment and the spermatogonial stem cell niche in man. J Proteome Res 13: 1259–1269.
75. Sharpe RM, Cooper I (1983) Testicular interstitial fluid as a monitor for changes in the intratesticular environment in the rat. J Reprod Fertil 69: 125–135.
76. Com E, Evrard B, Roepstorff P, Aubry F, Pineau C (2003) New insights into the rat spermatogonial proteome: identification of 156 additional proteins. Mol Cell Proteomics 2: 248–261.
77. Lavigne R, Becker E, Liu Y, Evrard B, Lardenois A, et al. (2012) Direct iterative protein profiling (DIPP) - an innovative method for large-scale protein detection applied to budding yeast mitosis. Mol Cell Proteomics 11: M111 012682.
78. Cote RG, Griss J, Dianes JA, Wang R, Wright JC, et al. (2012) The PRoteomics IDEntification (PRIDE) Converter 2 framework: an improved suite of tools to facilitate data submission to the PRIDE database and the ProteomeXchange consortium. Mol Cell Proteomics 11: 1682–1689.
79. Vizcaino JA, Cote R, Reisinger F, Barsnes H, Foster JM, et al. (2010) The Proteomics Identifications database: 2010 update. Nucleic Acids Res 38: D736–742.
80. Sayers EW, Barrett T, Benson DA, Bolton E, Bryant SH, et al. (2012) Database resources of the National Center for Biotechnology Information. Nucleic Acids Res 40: D13–25.
81. Altenhoff AM, Schneider A, Gonnet GH, Dessimoz C (2011) OMA 2011: orthology inference among 1000 complete genomes. Nucleic Acids Res 39: D289–294.
82. Com E, Rolland AD, Guerrois M, Aubry F, Jegou B, et al. (2006) Identification, molecular cloning, and cellular distribution of the rat homolog of minichromosome maintenance protein 7 (MCM7) in the rat testis. Mol Reprod Dev 73: 866–877.

BMC Genomics

RESEARCH ARTICLE Open Access

Testis transcriptome analysis in male infertility: new insight on the pathogenesis of oligo-azoospermia in cases with and without AZFc microdeletion

Valentina Gatta[†1,2], Florina Raicu[†3,4], Alberto Ferlin[†5], Ivana Antonucci[1,2], Anna Paola Scioletti[2,4], Andrea Garolla[5], Giandomenico Palka[1,6], Carlo Foresta[5] and Liborio Stuppia[*1,2,7]

Abstract

Background: About 10% of cases of male infertility are due to the presence of microdeletions within the long arm of the Y chromosome (Yq). Despite the large literature covering this critical issue, very little is known about the pathogenic mechanism leading to spermatogenesis disruption in patients carrying these microdeletions. In order to identify the presence of specific molecular pathways leading to spermatogenic damage, testicular gene expression profiling was carried out by employing a microarray assay in 16 patients carrying an AZFc microdeletion or affected by idiopathic infertility. Hierarchical clustering was performed pooling the data set from 26 experiments (16 patients, 10 replicates).

Results: An intriguing and unexpected finding is that all the samples showing the AZFc deletion cluster together irrespectively of their testicular phenotypes. This cluster, including also four patients affected by idiopathic infertility, showed a downregulation of several genes related to spermatogenesis that are mainly involved in testicular mRNA storage. Interestingly, the four idiopathic patients present in the cluster showed no testicular expression of *DAZ* despite the absence of AZFc deletion in the peripheral blood.

Conclusions: Our expression profiles analysis indicates that several forms of infertility can be triggered by a common pathogenic mechanism that is likely related to alterations in testicular mRNA storage. Our data suggest that a lack of testicular DAZ gene expression may be the trigger of such mechanism. Furthermore, the presence of AZFc deletions in mosaic or the loss of function of AZFc genes in absence of Yq deletion can perhaps explain these findings. Finally, based on our data, it is intriguing to hypothesize that *DAZ* gene dysfunctions can account for a larger number of previously thought "idiopathic" infertility cases and investigation of such testicular gene dysfunction can be important to reveal the molecular determinant of infertility than are undetected when only testing Yq deletions in peripheral blood.

Background

Microdeletions of the Y chromosome long arm (Yq) represent the main molecular determinants of male infertility and account for about 10% of cases of non obstructive azoospermia or severe hypospermatogenesis [1-5]. Yq microdeletions involve three Azoospermia Factors (AZF) loci, AZFa, AZFb and AZFc [6] and remove many genes likely involved in male germ cell development and maintenance [7]. The most frequent deletion of the Y chromosome (AZFc, b2/b4) spans 3.5 Mb and eliminates 21 genes and transcription units of the AZFc region. Among these, the main candidate for spermatogenesis failure is the Deleted in Azoospermia (DAZ) gene, a testis specific gene present in four copies within AZFc and encoding for an RNA binding protein [6,7]. The AZFc deletion has been associated with wide range of phenotypes ranging

* Correspondence: stuppia@unich.it
[1] Department of Biomedical Sciences, "G. d'Annunzio" University, Chieti-Pescara, Italy
[†] Contributed equally
Full list of author information is available at the end of the article

from the complete absence of germ cells in the testes (Sertoli cell only syndrome, SCOS) to a relevant reduction of germ cells still including mature sperm (severe hypospermatogenesis, HS), to a maturation spermatogenesis arrest. Despite the large number of studies investigating the prevalence and the molecular basis of these rearrangements, the testicular gene expression of patients carrying Yq deletions is still largely unknown and so are the molecular mechanisms leading to spermatogenesis disruption.

In recent years, expression profiling of human testis has been widely used for the identification of genes that are involved in different key steps of testis development and function [8-10]. However, at the moment, not a single study has investigated the testicular transcriptome of patients who carry Yq microdeletions.

In this study, we analyzed testis expression profiles of 16 infertile patients with different testicular phenotypes, including men carrying AZFc deletions as well as subjects with idiopathic infertility.

Results

In order to discriminate the genes specifically involved in the different pathological phenotypes, we performed a hierarchical clustering of the data set originated from 26 experiments (16 patients, 10 technical replicates) (Table 1). All the AZFc samples clustered together independently from their testis phenotype (SCOS or HS) (Figure 1). The same cluster also contained 4 patients without Yq deletions (3 affected by idiopathic HS and one by idiopathic SCOS). The remaining three patients without Yq deletions showed a different gene expression profile which was not clustered together with AZFc deleted patients. All the testes with normal spermatogenesis clustered appropriately into their group. The cluster containing AZFc-deleted samples was characterized by the presence of 490 transcripts showing at least a 1.7-fold change in expression as compared to testis with normal spermatogenesis (Additional file 1 and 2). Semiquantitative RT-PCR, carried out on selected genes (*ACTL7B, LDHC, ODF 1, TSSK2, PRM2, TNP1*), confirmed microarray results (additional file 3).

Ingenuity Pathway Analysis (IPA) was carried out to investigate the main functions played by genes that were found to be downregulated (n. = 331, additional file 1) and showed that "Cellular development" and "Reproductive system development and function" were the main functions correlated with these genes (Figure 2). These functional categories contained several genes playing a role in spermatogenesis, fertilization, and determination of the testicular mass, some of which are involved in human and murine male infertility (DDX25 and FKBP6) [11] (SPAG6) [12] (Table 2).

When we analyzed the upregulated genes (n = 159, additional file 2), IPA showed that "Cellular growth and proliferation" and "Cell death" were the functions to be involved, whereas "Reproductive system development and function" was less represented (Figure 3, Table 3).

Network analysis of the dowregulated genes that are linked with spermatogenesis showed an interesting network centered on the *YBX2* (*MSY2*) gene, a member of the Y-box gene family that is selectively expressed in male and female germ cells (Figure 4) [13]. We also found an additional network that is centered on the *ARNT2* gene and contains other genes critically involved in the spermatogenetic process (*CRISP2, TSSK2, MDM4* and *EGR4*) (Figure 5).

A specific analysis of the DAZ gene signal in the samples represented in the cluster showed that *DAZ* was not expressed in all the four patients who were not carrying the AZFc deletion (Table 4). These results were confirmed by a RT-PCR analysis carried out as previously described [14]. The same kind of analysis was carried out also for CDY1 and VCY2 genes, mapped in multiple copies within AZFc locus close to the DAZ gene cluster [7]. This analysis evidenced CDY1 expression in patients with idiopathic infertility but not in those with AZFc deletion. On the other hand, an overexpression of VCY2 gene was detected in 4 out of 6 patients with AZFc deletion. A BLAST search using the VCY2 oligonucleotide sequence spotted on the array discovered a 60% homology with the sequence mapped in Yp, corresponding to a portion of the VCY2 exon 7, in addition to the expected 100% homology with VCY2 coding region.

Discussion

In the present study, we carried out a microarray analysis to investigate testicular gene expression profiles in patients affected by different forms of infertility. Due to the absence or reduced number of germ cells in these patients, a downregulation of genes with prominent or exclusive germ cell expression was expected in all samples, whereas genes expressed mainly in somatic cells were expected to show increased expression. However, the main purpose of this study was to analyze the inter-individual differences among infertile patients, in order to identify specific expression profiles for each different conditions.

Using this approach we found a similar gene expression profile in all the samples originated from individuals carrying the AZFc deletion as well as in four patients with idiopathic infertility. All these case showed a common gene cluster that contained 490 transcripts (331 down- and 159 upregulated genes). Since all HS patients had the same Johnsen score, the difference in the expression profiles of samples present in the cluster and patients outside

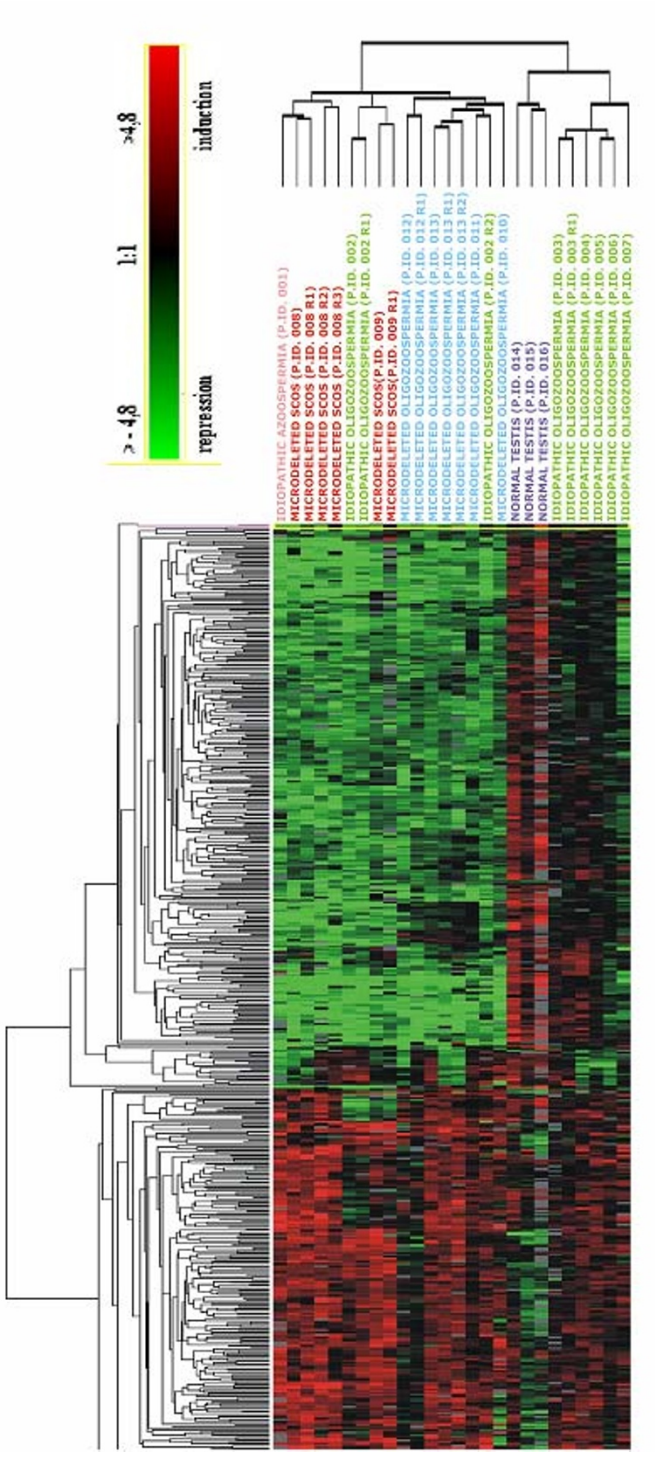

Figure 1 Hierarchical clustering showing a similar expression profile in all patients with AZFc deletions and in four patients with idiopathic infertility. In the figure, all the relevant genes are grouped according to their expression values shown as log ratios (ratios are: gene expression value of the pathological testis divided by the value of a normal testis and values of the three samples with normal spermatogenesis divided by the home-made RNA universal). Each row corresponds to one gene, each column to different 26 microarray experiments. The quantitative changes in gene expression across all the samples are represented in color: red indicates overexpressed genes, and green indicates downregulated genes. Black bars indicate no changes in expression. Missing data points are represented as gray bars. Different colors of top labels indicate different testis phenotypes. (Pink= idiopathic SCOS; red = AZFc microdeletion with SCOS phenotype; green = idiopathic HS; blue = AZFc microdeletion with HS phenotype; purple = normal testis; R= replica).

Table 1: Testis phenotype of the investigated patients and number of micorarray experiments.

Patients classification	Semen analysis	Testis histology (Johnsen score)	Patient ID	Microarray experiments
Idiopathic SCOS	Azoospermia	SCOS (2)	1	1
Idiopathic HS	$\leq 1 \times 10^6$/ml	Severe HS (8)	2	3
			3	2
			4	1
			5	1
			6	1
			7	1
AZFc microdeletion SCOS	Azoospermia	SCOS (2)	8	4
			9	2
AZFc microdeletion HS	$\leq 1 \times 10^6$/ml	Severe HS (8)	10	1
			11	1
			12	2
			13	3
Obstructive azoospermia	Azoospermia	Normal spermatogenesis (10)	14	1
			15	1
			16	1
Total microarray experiments				26

the cluster cannot be due to a different number of germ cells in their testis, but likely indicates a real difference in the transcription levels of specific genes. Among the downregulated transcripts, we detected several genes involved in spermatogenesis, fertilization, and male infertility. To clarify a potential pathogenic link between the downregulation of these transcripts and spermatogenesis failure, we carried out an IPA network analysis that revealed two interesting networks. The first network is centered on the YBX2 (MSY2) gene, a member of the Y-box gene family that is specifically expressed in male and female germ cells. *YBX2* marks specific mRNAs for cytoplasmic storage, stabilization, and suppression of translation [13]. RNA storage is a crucial step during spermatogenesis. RNA synthesis terminates during mid-spermiogenesis and stabilization and storage of mRNAs are key for the encoding of proteins needed during the terminal phases of spermatogenesis [15]. Quite surprisingly, network analysis of the cluster of patients carrying AZFc deletions showed that *YBX2* was not present in the cluster, being not significantly downregulated in the samples within the cluster as compared to the other samples not present in the cluster. However, several genes whose activity is regulated by *YBX2* were found to be downexpressed in the network. Among these, we found *ODF1, TNP1* and *PRM2*, all genes that play a key role in the postmeiotic phase of the spermatogenesis. ODF1 encodes for proteins located on the outside of the axoneme in the mid piece and principal piece of the mammalian sperm tail, thereby maintaining the passive elastic structures and elastic recoil of the sperm tail. TNP1 is a spermatid-specific product of the haploid

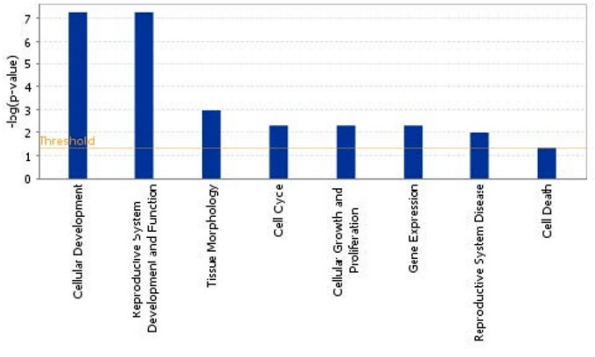

Figure 2 Histogram showing the main biological functions of downregulated genes present in the cluster of patients with AZFc deletion.

Table 2: Dowregulated genes in the cluster containing AZFc deleted samples as classified on the basis of their main biological functions.

General biological function	Specific biological function	Downregulated genes in AZFc deleted patients cluster
Cellular development	Spermatogenesis	AFF4, CCT6B, CRISP2, DDX25, FKBP6, KIF6, PRM2, SPAG6, TNP1, TSGA10
Reproductive system development and function	Fertilization	CLGN, DAZ1, TNP1, PCSK4
	Mass of testis	ARL4A, PTDSS2

genome which replaces histones and is itself replaced in the mature sperm by the protamines. *PRM2* encodes for proteins playing a key role in DNA packaging during sperm differentiation. The combined downregulation of all these genes suggests reduced storage of these transcripts during spermatogenesis, via a *YBX2*-independent process as the *YBX2* transcript was not found within the cluster. A possible intriguing hypothesis is that the loss of function of the *DAZ* gene, the most important gene disrupted by AZFc deletions [16], leads to a pathogenic defective mRNA storage. Substantiating this idea, RNA-binding proteins encoded by *DAZ* are known to be required for the translational regulation of gene expression that is essential for gametogenesis [17,18]. Furthermore, it has been showed that *Dazl*, the murine homologous of *DAZ*, plays a role in the transport of specific mRNAs via a dynein motor complex, and that the *Dazl*-bound mRNAs is stored at specific sites to be available and used for later developmental processes [19]. Therefore we hypothesize that *DAZ* disruption may represent a possible cause of the reduced storage of important testis transcripts encoded in the first steps of the spermatogenesis.

Interestingly, the second network we analyzed is centered on the *ARNT2* gene and contains several genes involved in the spermatogenesis process (*CRISP2, TSSK2, MDM4* and *EGR4*). *CRISP2* is a testis-enriched protein localized to the sperm acrosome and tail. *TSSK2* encodes a testis-specific serine/threonine kinase and is bound by the human and murine forms of DAZL. EGR4 is a member of the *Egr* family of zinc-finger transcription factors, and regulates genes critically involved in the early stages of meiosis. Thus, it is intriguing to conceive that also *ARNT2* may play an important role in the pathogenesis of infertility in AZFc deleted patients.

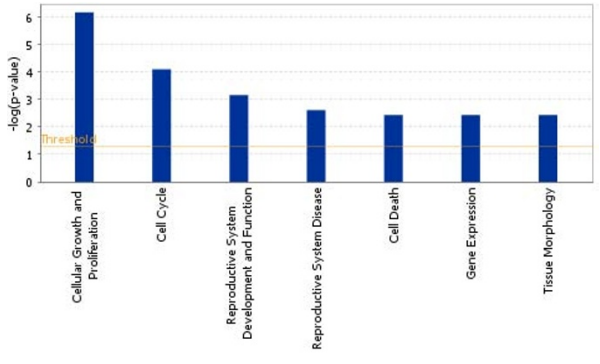

Figure 3 Histogram showing the main biological functions of up-regulated genes present in the cluster of patients with AZFc deletion.

The microarray analysis of samples from patients with AZFc deletion also showed the presence of 159 upregulated transcripts. It is interesting to note that only a few of these genes have been previously linked to infertility. *A2M*, a gene that is encoding for a protease inhibitor, is up-regulated in the testis of the ABP transgenic mouse that shows an impairment of spermatogenesis [20]. Increased expression of *HIF1A*, an hypoxia-inducible transcription factor, is present in the internal spermatic vein of patients with varicocele [21]. Finally, *HMGB1*, encoding for a high mobility group protein, works as a pro-inflammatory and antibacterial factor in human testis [22]. These data suggest that the overexpression of genes related to cell growth and proliferation as well as to apoptosis in the testis of patients with AZFc deletions may represent an unspecific mechanism of reaction to testis damage, rather than the cause of defective spermatogenesis.

An unexpected finding of the present study is that the four patients without AZFc deletion are included in the same cluster containing samples from AZFc deleted patients. In order to verify if the presence of an intact AZFc region in peripheral blood actually correlates with a normal testicular DAZ expression, we focused our attention to the presence/absence of the specific signals for this gene on the array in all cases contained in the cluster. Interestingly, no DAZ signal was detected in any of the four patients without AZFc deletion. Lack of DAZ expression was expected in the samples from patients affected by idiopathic SCOS, due to the absence of germ cells, but it was surprisingly found in the 3 patients affected by idiopathic HS.

The lack of *DAZ* expression in the testis of infertile patients who are not carrying the AZFc deletion in their peripheral blood has been previously reported and inter-

Table 3: Upregulated genes in the cluster containing AZFc deleted samples as classified on the basis of their main biological functions.

General biological function	Specific biological function	Upregulated genes in AZFc deleted patients cluster
Cellular growth and proliferation	Proliferation of eucariothic cell	A2M, ADAMTS1, AIF1, ANGPTL1, CEBPD, COL4A1, DCN, GSTM1, HIF1A, HMGB1, ICMT, IL6ST, KIF3A, LY96, NKX3-1, PLAU, PTK2, S100B, SOD2, SPTBN1, TPT1
Reproductive system development and function	Reproductive process of mammalia	DDX3Y (DBY), IL6ST, PLAU, UTY
Cell death	apoptosis of eukaryotic cells	A2M, ANGPTL1, C7, CEBPD, DCN, HIF1A, HMGB1, ICMT, IL6ST, KIF3A, PLAU, PTK2, SOD2, TPT1, YES1

preted as the result of somatic AZFc rearrangements producing a mosaic in which Yq deletion is present only in testicular cells [14,23]. Our results strongly confirm this finding, corroborating the hypothesis that a portion of patients classified as affected by idiopathic infertility actually lack DAZ gene expression in their testis, thus showing a pathogenic mechanism similar to the one responsible of infertility in AZFc deleted patients. In order to investigate also other AZFc genes, we analyzed the specific spots for CDY1 and VCY2, in order to verify their expression in patients with and without AZFc deletion. As expected, CDY1 was expressed in infertile patients without AZFc deletion independently fromtheir collocation with or without the cluster, but not in patients with AZFc deletion. On the other hand, expression levels showed by VCY2 gene were inconsistent with those of DAZ and CDY1 genes, being this gene overexpressed in 4 out of the 6 patients with AZFc deletion. In order todisclose the cause of this unexpected result, we performed a Blast search using the VCY2 oligonucleotide sequence spotted on the array, discovering a 60% homology with a sequence mapped within Yp, in addition of the expected 100% homology with VCY2 gene. This Yp sequence matched with the VCY2 exon 7, target of the VCY2 probe present in the array. On the other hand, DAZ and CDY1 probes showed homology only with their target genes. This suggests that the VCY2 oligonucleotide on the array is not specific enough to consider the expression levels of this gene in the context of the present study.

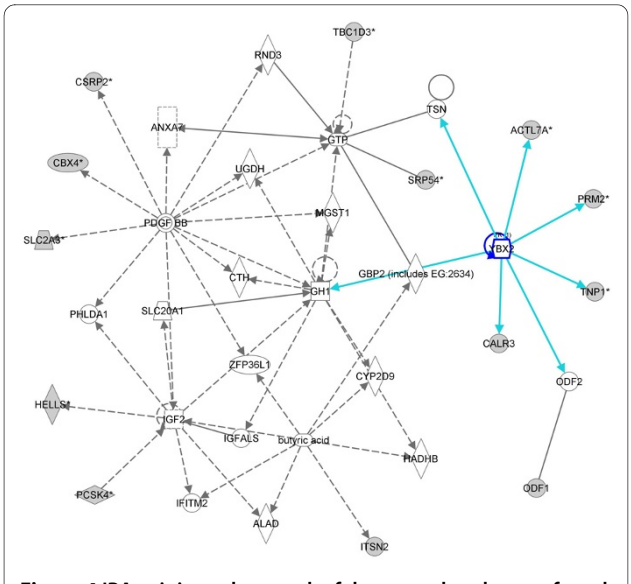

Figure 4 IPA-originated network of downregulated genes found in the cluster of patients with AZFc deletion. Network centered on YBX2 gene. The grey shading indicates genes that show decreased expression in the pathological testis when compared with normal testis samples.

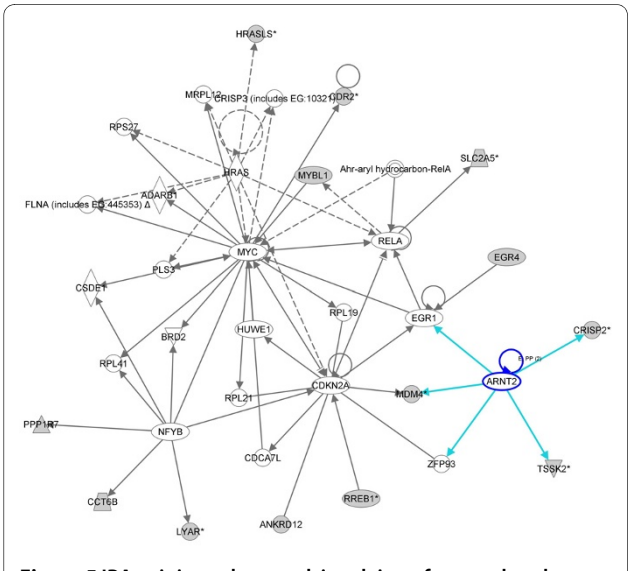

Figure 5 IPA-originated network involving of upregulated genes found in the cluster of patients with AZFc deletion. Network centered on ARNT2 gene. The grey shading indicates genes that show increased expression in the pathological testis when compared with normal testis samples.

Table 4: Expression of the DAZ gene in the investigated patients as evidenced by microarray analysis. + = presence of expression. - = absence of expression.

Patient ID	Phenotype	Present in the cluster	DAZ expression
1	Idiopathic SCOS	Yes	-
2	Idiopathic HS	No	+
3	Idiopathic HS	No	+
4	Idiopathic HS	No	+
5	Idiopathic HS	Yes	-
6	Idiopathic HS	Yes	-
7	Idiopathic HS	Yes	-
8	AZFc deletion SCOS	Yes	-
9	AZFc deletion SCOS	Yes	-
10	AZFc deletion HS	Yes	-
11	AZFc deletion HS	Yes	-
12	AZFc deletion HS	Yes	-
13	AZFc deletion HS	Yes	-
14	Normal spermatogenesis	No	+
15	Normal spermatogenesis	No	+
16	Normal spermatogenesis	No	+

Conclusions

In summary, our study provides the following novel information: i) all patients with AZFc deletions show a similar testis gene expression profile, independently from their SCOS or HS phenotype, suggesting that all AZFc deletions produce a similar transcriptional pattern and that variability in phenotypes is related to environmental or other genetic mechanisms. ii) one half of the patients with idiopathic infertility cluster together with patients with AZFc deletions, suggesting a common pathogenic mechanism. We hypothesize that a crucial link that can explain this phenomenon is the lack of expression of the *DAZ* gene in the testes these cases. A potential alternative explanation may be related to the presence of an AZFc deletion in mosaic and/or the loss of function of AZFc genes in absence of Yq deletion. If our finding will be confirmed on larger series of patients, *DAZ* gene dysfunctions may be proved to account for a larger portion of cases of infertility than one could expect by simply analyzing the prevalence of Yq deletions among these subjects; iii) we found that several genes that are mainly related to the postmeiotic phase of the spermatogenesis and have been previously reported as involved in male infertility are dowregulated in patients with AZFc deletions. Given the crucial role played by RNA storage during spermatogenesis, the loss of function of *DAZ* can translate to a defective mRNA storage in testis with great pathogenic implications. The identification of the molec-

ular mechanisms underlying the spermatogenesis failure in cases characterized by DAZ loss of function will provide useful information for the disclosure of key molecules which could represent in the future the target for personalized drug therapy.

Methods

Patients

The study was approved by the local Ethics Committee of the University of Padova and was in accordance with the Helsinki II Declaration. All participants were asked for and provided their informed consent. The study population was selected from a cohort of 1436 men presenting idiopathic non obstructive azoospermia or severe hypospermatogenesis (sperm count <2 million/ml) [5]. Exclusion criteria were: drug consumption, fever in the previous 6 months, seminal infections, varicocele, systemic diseases, previous cryptorchidism or orchitis, presence of anti-sperm auto-antibodies, hypogonadotrophic hypogonadism, abuse of androgenic (anabolic) steroids, treatment with chemotherapeutic agents or radiotherapy, testicular tumors, karyotype abnormalities, androgen receptor, INSL3 and RXFP2 gene mutations [24,25]. Semen analysis was performed according to the World Health Organization guidelines [26] on at least two occasions separated by three months. The diagnosis of azoospermia was established by pellet analysis after semen centrifugation.

The testicular structure and spermatogenic activity was evaluated with a combination of methods to have the most homogeneous sampling. As a screening procedure, bilateral testicular fine needle aspiration (FNA) was performed as previously described [5,27]. Testicular phenotype was classified as follows (1) Sertoli cell only syndrome (SCOS): complete absence of all germ cells in both testes; (2) hypospermatogenesis (HS): quantitative reduction in the number of germs cells with still presence of mature spermatozoa; and (3) maturation arrest (MA): normal presence of germ cells until a definite step of spermatogenesis and lack of germ cells in the later stages.

Patients showing normal karyotype were submitted to molecular testing for Yq microdeletions as previously described (5). Only men carrying the AZFc-b2/b4 deletion were included in the microarray analysis.

The final selected sample comprised 16 patients (pats. 1-16): one patient (pat. 1) had idiopathic SCOS, 6 patients (pats. 2-7) had idiopathic severe HS, 3 patients (pats. 8-10) had SCOS and AZFc-b2/b4 deletion, and 3 patients (pats. 11-13) had severe HS and AZFc-b2/b4 deletion. Three men with obstructive azoospermia and normal spermatogenesis were used as controls (pats. 14-16) (Tab. 1).

Testicular histology

Selected subjects underwent bilateral testicular biopsy to clearly assess testicular histology and provide RNA for microarray experiments. At least three 3-5 mm fragments per testis were excised, processed for histological analysis, and at least one sample per testis was submerged in 2 ml of RNAlater (Ambion, Austin, TX, USA). Only biopsy specimens showing a homogeneous histopathology of the testis parenchyma and samples yielding high-quality total RNA preparation were included in the analysis. Testicular histology was classified using a modification of the classical scoring procedure employed by Johnsen [28] as: (1) biopsies obtained from patients with post-testicular obstructions showing complete spermatogenesis, i.e. all stages represented and >20 late spermatids (also referred as "testicular spermatozoa") per seminiferous tubule (score count 10); (2) biopsies showing severe HS in all seminiferous tubules (score count 8); (3) biopsies from patients with SCOS (score count 2).

Microarray analysis

Testis samples were homogenized using an hand glass potter, and total testis RNA extracted using the *SVtotal RNA Izolation System* kit (Promega, Madison, WI, USA). The purity and quantity of RNA was assessed using the Agilent 8453 Spectrophotometer (Agilent, Santa Clara, CA, USA). RNA quality was determined by both evaluation of the integrity of rRNA bands using agarose electrophoresis, and absorbtion readings at 260 and 280 nm. Extracted RNA was linearly amplified using the *Amino Allyl MessageAmp™ II aRNA Amplification Kit* (Ambion, Austin, TX, USA).

Five to ten ug of amplified aRNA was fluorescently labelled with Cy3-Cy5 cyanins and then hybridizated on high-density array (Microcribi Padova, Italy). The Human Array Ready Oligo Set Version 2 contains array able 70mers representing 21,329 well-characterized human genes in two replicates from the UniGene Database. This database is located at the National Center for-Biotechnology Information (see http://www.ncbi.nlm.nih.gov/UniGene/). The UniGene database automatically clusters all human GenBank sequences into a non-redundant set of genes. Each cluster in the UniGene Database represents one unique gene. A cluster may contain manysequences, but one representative sequence has been selected based on the longest region of high-quality sequence data. All pathological testis RNAs were hybridized against normal testis RNA samples (patients with obstructive azoospermia and normal spermatogenesis) while the three samples with normal spermatogenesis were hybridized against an homemade RNA universal reference (brain, liver, muscle and

lung), to generate a profile of genes specifically expressed in normal testis, for a total of 26 experiments (tab. 1). After hybridization, Cy3-Cy5 fluorescent signals were captured by a Confocal Laser Scanner "ScanArray Express" (Packard BioScience) and analysed using the software "ScanArray Express - MicroArray Analysis System" version *3.0* (Perkin Elmer). Raw data of the performed experiments have been recorded in the GEO public database (accession number: GSE14310).

The values of the median signal intensity from each spot were subtracted from the local median background intensity. For each slide after local background subtraction, a LOWESS algorithm was used for row data normalization to evaluate signal to noise ratio and generate log ratios of sample vs. reference signal. Only spots showing a signal to noise ratio of at least 1.7 were included in the analysis.

Analysis of data obtained by microarray experiments was carried out by means of hierarchical gene clustering [29] using Cluster 3.0 (open source 2006) and TreeView (Stanford University Labs) software. In order to include in clustering analysis only well measured transcripts, we selected spots with a present call (identified transcripts with measurable expression) in at least 80% of experiments and being > 1.7 fold up- or down regulated in at least 8 experiments. Identified clusters were then analyzed by the Ingenuity Pathways Analysis (IPA) software (Ingenuity Systems, Redwood City, CA), in order to classify genes based on their biological functions and disclose the functional networks connecting specific genes.

Web Resources

Microarray data are deposited in the GEO public database and are accessible without restriction at the following URL: http://www.ncbi.nlm.nih.gov/geo/query/acc.cgi?token=bhqhdyekysokofq&acc=GSE14310 (accession number: GSE14310).

Additional material

Additional file 1 List of transcripts (along with their relative accession numbers), that are found downregulated in the cluster of patients with AZFc deletion.

Additional file 2 List of transcripts (along with the relative accession number) that are found upregulated in the cluster of patients with AZFc deletion.

Additional file 3 Semiquantitative RT-PCR analysis of 6 major genes downregulated in pathological testis. The housekeeping gene (GADPH: NP_002037.2) was used as control. 34 and 35 indicate the number of PCR cycles.

Competing interests

The authors declare that they have no competing interests.

Authors' contributions

Study design VG, AF, CF, LS; Patients selection: AF, AG, CF, GP; Gene expression analysis: VG, FR, APS; RT-PCR analysis: FR, IA; Manuscript writing: VG, AF, GP, LS. All authors read and approved the final manuscript.

Acknowledgements

This study was supported by grants from the Italian Ministry of University and Research (to CF and GP), the University of Chieti (to VG, GP and LS) and the University of Padova (to AF and CF).

The authors are grateful to Stefano L. Sensi for critical reading of the manuscript.

Grant support: This study was supported by grants from the Italian Ministry of University and Research (to CF and GP), the University of Chieti (to VG, GP and LS) and the University of Padova (to AF and CF).

Author Details

[1]Department of Biomedical Sciences, "G. d'Annunzio" University, Chieti-Pescara, Italy, [2]Aging Center Research, "G. d'Annunzio" Foundation, Chieti-Pescara, Italy, [3]Carol Davila University of Medicine and Pharmacy, Genetics Chair, Bucharest, Romania, [4]Department of Clinical Sciences and Imaging, "G. d'Annunzio" University, Chieti-Pescara, Italy, [5]Centre for Male Gamete Cryopreservation, Department of Histology, Microbiology, and Medical Biotechnologies, University of Padova, Italy, [6]Human Genetics Division, "Spirito Santo" Hospital, Pescara, Italy and [7]IGM-CNR c/o IOR, Bologna, Italy

Received: 18 December 2009 Accepted: 24 June 2010
Published: 24 June 2010

References

1. Stuppia L, Gatta V, Calabrese G, Guanciali Franchi P, Morizio E, Bombieri C, Mingarelli R, Sforza V, Frajese G, Tenaglia R, Palka G: **A quarter of men with idiopathic oligo-azoospermia display chromosomal abnormalities and microdeletions of different types in interval 6 of Yq11.** *Hum Genet* 1998, **102(5):**566-70.
2. McElreavey K, Krausz C: **Sex Chromosome Genetics '99. Male infertility and the Y chromosome.** *Am J Hum Genet* 1999, **64(4):**928-33.
3. Foresta C, Moro E, Ferlin A: **Y chromosome microdeletions and alterations of spermatogenesis.** *Endocrine Reviews* 2001, **22:**226-329.
4. Ferlin A, Raicu F, Gatta V, Zuccarello D, Palka G, Foresta C: **Male infertility: role of genetic background.** *Reprod Biomed Online* 2007, **14(6):**734-45.
5. Ferlin A, Arredi B, Speltra E, Cazzadore C, Selice R, Garolla A, Lenz A, Foresta C: **Molecular and clinical characterization of Y chromosome microdeletions in infertile men: a 10-year experience in Italy.** *J Clin Endocrinol Metab* 2007, **92(3):**762-70.
6. Vogt PH, Edelmann A, Kirsch S, Henegariu O, Hirschmann P, Kiesewetter F, Kohn FM, Schill WB, Farah S, Ramos C, Hartmann M, Hartschuh W, Meschede D, Behre HM, Castel A, Nieschlag E, Weidner W, Grone HJ, Jung A, Engel W, Haidl G: **Human Y chromosome azoospermia factors (AZF) mapped to different subregions in Yq11.** *Hum Mol Genet* 1996, **5(7):**933-43.
7. Kuroda-Kawaguchi T, Skaletsky H, Brown LG, Minx PJ, Cordum HS, Waterston RH, Wilson RK, Silber S, Oates R, Rozen S, Page DC, Curoda-Kawaguchi T: **The AZFc region of the Y chromosome features massive palindromes and uniform recurrent deletions in infertile men.** *Nat Genet* 2001, **29(3):**279-86.
8. Ostermeier GC, Dix D, Miller D, Khatri P, Krawetz SA: **Spermatozoal RNA profiles of normal fertile men.** *The Lancet* 2002, **360:**772-777.
9. He Z, Chan WY, Dym M: **Microarray technology offers a novel tool for the diagnosis and identification of therapeutic targets for male infertility.** *Reproduction* 2006, **132:**11-19.
10. Okada H, Tajima A, Shichiri K, Tanaka A, Tanaka K, Inoue I: **Genome-wide expression of azoospermia testes demonstrates a specific profile and implicates ART3 in genetic susceptibility.** *PLoS Genet* 2008, **4(2):**e26.
11. Zhang AZ, Yang SY, Ma Y, Lin L, Zhang W: **Single nucleotide polymorphisms of the gonadotrophin-regulated testicular helicase (GRTH) gene may be associated with the human spermatogenesis impairment.** *Hum Reprod* 2006, **21(3):**755-9.
12. Sapiro R, Kostetskii I, Olds-Clarke P, Gerton GL, Radice GL, Strauss JF III: **Male infertility, impaired sperm motility, and hydrocephalus in mice deficient in sperm-associated antigen 6.Mol.** *Cell Biol* 2002, **22(17):**6298-305.
13. Yang J, Morales CR, Medvedev S, Schultz RM, Hecht NB: **In the absence of the mouse DNA/RNA-binding protein MSY2, messenger RNA instability leads to spermatogenic arrest.** *Biol Reprod* 2007, **76(1):**48-54.

14. Ferlin A, Moro E, Onisto M, Toscano E, Bettella A, Foresta C: **Absence of testicular DAZ gene expression in idiopathic severe testiculopathies.** *Hum Reprod* 1999, **14(9):**2286-92.
15. Hecht NB: **Molecular mechanisms of male germ cell differentiation.** *BioEssays* 1998, **20:**555-561.
16. Reijo R, Lee TY, Salo P, Alagappan R, Brown LG, Rosenberg M, Rozen S, Jaffe T, Straus D, Hovatta O, de la Chapelle A, Silber S, Page DC: **Diverse spermatogenic defects in humans caused by Y chromosome deletions encompassing a novel RNA-binding protein gene.** *Nat Genet* 1995, **10:**383-39.
17. Collier B, Gorgoni B, Loveridge C, Cooke HJ, Gray NK: **The DAZL family proteins are PABP-binding proteins that regulate translation in germ cells.** *EMBO J* 2005, **24(14):**2656-66.
18. Reynolds N, Collier B, Maratou K, Bingham V, Speed RM, Taggart M, Semple CA, Gray NK, Cooke HJ: **Dazl binds in vivo to specific transcripts and can regulate the pre-meiotic translation of Mvh in germ cells.** *Hum Mol Genet* 2005, **14(24):**3899-909.
19. Lee KH, Lee S, Kim B, Chang S, Kim SW, Paick JS, Rhee K: **Dazl can bind to dynein motor complex and may play a role in transport of specific mRNAs.** *EMBO J* 2006, **25(18):**4263-70.
20. Petrusz P, Jeyaraj DA, Grossman G: **Microarray analysis of androgen-regulated gene expression in testis: the use of the androgen-binding protein (ABP)-transgenic mouse as a model.** *Reprod Biol Endocrinol* 2005, **3:**70.
21. Lee JD, Jeng SY, Lee TH: **Increased expression of hypoxia-inducible factor-1alpha in the internal spermatic vein of patients with varicocele.** *J Urol* 2006, **175(3 Pt 1):**1045-8.
22. Zetterström CK, Strand ML, Söder O: **The high mobility group box chromosomal protein 1 is expressed in the human and rat testis where it may function as an antibacterial factor.** *Hum Reprod* 2006, **21(11):**2801-9.
23. Song NH, Yin CJ, Zhang W, Zhuo ZM, Ding GX, Zhang J, Hua LX, Wu HF: **AZF gene expression analysis in peripheral leukocytes and testicular cells from idiopathic infertility.** *Arch Androl* 2007, **53(6):**317-24.
24. Ferlin A, Bogatcheva NV, Gianesello L, Pepe A, Vinanzi C, Agoulnik AI, Foresta C: **Insulin-like factor 3 gene mutations in testicular dysgenesis syndrome: clinical and functional characterization.** *Mol Hum Reprod* 2006, **12:**401-6.
25. Ferlin A, Vinanzi C, Garolla A, Selice R, Zuccarello D, Cazzadore C, Foresta C: **Male infertility and androgen receptor gene mutations: clinical features and identification of seven novel mutations.** *Clin Endocrinol (Oxf)* 2006, **65:**606-10.
26. World Health Organization: **WHO laboratory manual for the examination of human semen and sperm-cervical mucus interaction.** Cambridge University Press, Cambridge UK; 1999.
27. Foresta C, Ferlin A, Bettella A, Rossato M, Varotto A: **Diagnostic and clinical features in azoospermia.** *Clin Endocrinol (Oxf)* 1995, **43:**537-43.
28. Johnsen SG: **Testicular biopsy score count--a method for registration of spermatogenesis in human testes: normal values and results in 335 hypogonadal males.** *Hormones* 1970, **1:**2-25.
29. Pasanen T, Saarela J, Saarikko I, Toivanen T, Tolvanen M, Vihinen M, Wong G: *DNA microarray data analysis* CSC - Scientific Computing Ltd, Finland; 1970.

doi: 10.1186/1471-2164-11-401
Cite this article as: Gatta *et al.*, Testis transcriptome analysis in male infertility: new insight on the pathogenesis of oligo-azoospermia in cases with and without AZFc microdeletion *BMC Genomics* 2010, **11**:401